Theory of Auger Ejection of Electrons from Metals by Ions

HOMER D. HAGSTRUM
Bell Telephone Laboratories, Murray Hill, New Jersey
(Received June 16, 1954)

Electrons ejected from atomically clean metals by slow ions of the noble gases arise in Auger transitions which involve either the direct neutralization of the ion or the de-excitation of an excited atom. A theory of these processes is presented in which the form of the distribution in energy and relative total yield, γ_i, of ejected electrons are derived. Matrix elements are not evaluated from first principles, but specific use of experimental results at two points in the theory leads to a determination of the dependence of the matrix element on distance between the atomic particle and the metal surface and the angle between the excited electron's velocity and the surface normal. Inclusion of the effects of variation of atomic energy levels near the metal surface and the Heisenberg uncertainty principle makes it possible to account in some detail for the experimentally observed energy distributions as well as the variation of these and of γ_i with ion kinetic energy. The effect upon the resonance ionization and neutralization processes of the variation of atomic energy levels near the metal surface has also been investigated. The theory predicts a critical distance from the metal surface outside which resonance neutralization and inside which resonance ionization are possible. It has also been possible for the specific case of noble gas ions on tungsten, used as an illustrative example, to determine the relative proportion of electrons ejected by each of the possible Auger processes, to estimate γ_i values for ions incident upon a metal with thermal energies, and to fix limits on the width of the filled portion of the conduction band in the metal. The role of the state density function in the metal and the effect of possible variation of the matrix element with electron energy in the band are also investigated.

I. INTRODUCTION

IT has been recognized for some time that electrons can be ejected from metals by slow ions of sufficiently large ionization energy. The Auger transitions in which these electrons are released do not involve directly the translational energy of the incoming particle. Two possible processes have been proposed and treated theoretically. After Oliphant and Moon[1] suggested the *resonance neutralization* of an ion at a metal surface by tunneling of an electron to populate an excited level, Massey,[2] Shekhter,[3] and Cobas and Lamb[4] have treated the two-stage process of *resonance neutralization* followed by electron ejection in *Auger de-excitation* of the excited atom. Shekhter[3] has also proposed and investigated theoretically the single process of electron ejection by *Auger neutralization* in which the ion is neutralized directly to the ground state. In each of these treatments the primary emphasis has been placed upon the calculation of the matrix elements and the determination of transition probability per unit time as a function of distance from the metal surface for such cases as H^+ or He^+ incident upon molybdenum.

Recent experimental work[5–7] involving noble gas ions incident on atomically clean metals has produced a number of results for which existing theory provides no explanation. The present work attempts to take account of the following effects not treated in the early theories:

1. the distribution of the participating electrons over the initial states in the metal (Secs. III and IV),
2. the dependence of the matrix element on angle which the excited electron's velocity makes with the surface normal (Secs. III and IV),
3. the probability that an excited electron will escape from the metal (Sec. VI),
4. the variation of atomic energy levels when the particle is near the metal surface (Secs. VIII, IX, and X),
5. the finite lifetime of the initial state of the system of metal and ion (Sec. XII), and
6. the role of the resonance processes in determining partition between Auger neutralization and de-excitation processes (Secs. XI and XIV).

No attempt is made in this work to evaluate matrix elements from first principles. However, two fits to the experimental data make it possible to evaluate the magnitude of the matrix element as a function of distance of the atomic particle from the surface and its dependence upon the angle between the excited electron's velocity and the surface normal (Sec. XIII).

For the case of noble gas ions on tungsten,[7] used as an illustrative example, it is possible to show that the Auger neutralization process accounts for all electrons ejected by very slow ions (<10 ev). At somewhat higher energies it is shown that only in the case of Ne^+ does the two-stage ejection process play any role. Even in this case a relatively small percentage of encounters (~ 10 percent) result finally in the Auger de-excitation process. With reasonable assumptions concerning the state density function in the conduction band of the metal and concerning the dependence of

[1] M. L. E. Oliphant and P. B. Moon, Proc. Roy. Soc. (London) **A127**, 388 (1930).
[2] H. S. W. Massey, Proc. Cambridge Phil. Soc. **26**, 386 (1930); **27**, 469 (1931).
[3] S. S. Shekhter, J. Exptl. Theoret. Phys. (U.S.S.R.) **7**, 750 (1937).
[4] A. Cobas and W. E. Lamb, Jr., Phys. Rev. **65**, 327 (1944).
[5] H. D. Hagstrum, Phys. Rev. **89**, 244 (1953).
[6] H. D. Hagstrum, Phys. Rev. **91**, 543 (1953).
[7] H. D. Hagstrum, preceding paper, Phys. Rev. **96**, 325 (1954).

the matrix element on initial energies of the participating electrons it has been possible to derive theoretical electron energy distributions and total yields which account for all the major features of the experimental results (Sec. XIV) and their dependences upon ion kinetic energy (Sec. XV). A reasonable extrapolation of the experimental results to the energy range of interest in gas discharges is now possible.

The theory of the resonance processes predicts that the distance between atomic particle and the metal surface must exceed a critical value for resonance neutralization to occur and must be less than this critical value for resonance ionization to occur (Sec. X). This situation further restricts the possibility of two-stage ejection but makes possible a three-stage process in the case of incident ions.

As might be expected the Auger processes considered here depend in an important way upon the electronic band structure of the metal involved. It appears possible to derive some information concerning the band structure from this work, in particular, concerning the energy levels of the top and bottom of the filled portion of the conduction band (Sec. XVI).

Notation used in this paper is defined in Table I. Energy values used are given in Table II. A general discussion of the processes which may occur as an ion or excited atom strikes a metal surface is included in the next section.

II. ELECTRONIC TRANSITIONS INVOLVING AN ION OR EXCITED ATOM NEAR A METAL SURFACE

In considering what can happen to an ion or excited atom as it approaches and strikes a metal surface it is convenient to distinguish electronic transitions which occur farther from the surface and involve principally the potential energy of the particle from processes which require much closer approach or actual penetration of the lattice and involve much more directly the kinetic energy of the particle. All evidence points to the conclusion that the electrons ejected from metals by slow ions of the noble gases arise in processes falling into the first of these categories. It is the purpose in this section to identify the basic electronic transitions and to discuss briefly the other possible interactions with the metal.

Electronic transitions in which an excited atom or ion near a metal surface could conceivably become involved are of the *resonance*, *Auger*, and *radiative* types. However, Shekhter[8] has shown that the probability of neutralization of an ion near a metal accompanied by radiation is very low ($\sim 5\times 10^{-7}$). The probability of any radiative process is expected to be low because the lifetime for radiation ($\sim 10^{-8}$ sec) is very long compared to the time which even a thermal particle spends within a few angstrom units of the surface ($\sim 10^{-12}$ sec). Ions and excited atoms near but not in intimate contact with a metal surface must thus undergo electronic changes in resonance- or Auger-type processes. Four basic electronic transitions may be distinguished. These are: 1. *resonance neutralization* of an ion, 2. *resonance ionization* of an atom, 3. *Auger neutralization* of an ion, and 4. *Auger de-excitation* of an excited atom. These processes are illustrated schematically in Figs. 1, 2, and 3, in which the energy levels shown are approximately those appropriate to He and tungsten.

It would appear that kinetic energy of the atomic particle can play no role in the transitions of Figs. 1, 2, and 3. When account is taken of energy level shifts near the metal surface, however, it becomes possible for some kinetic energy to be involved by first being transformed into potential energy in the interaction field near the surface.

Of the processes which require more intimate contact with the metal those in which electrons are released are of primary interest here. There appear to be three possible means of kinetic ejection of electrons.[8] These are: 1. acceleration of nearly free electrons inside the metal,[9,10] 2. thermal emission of electrons by local heating,[11–13] and 3. release of bound electrons from atoms at the surface or in the interior of the metal.[8,14]

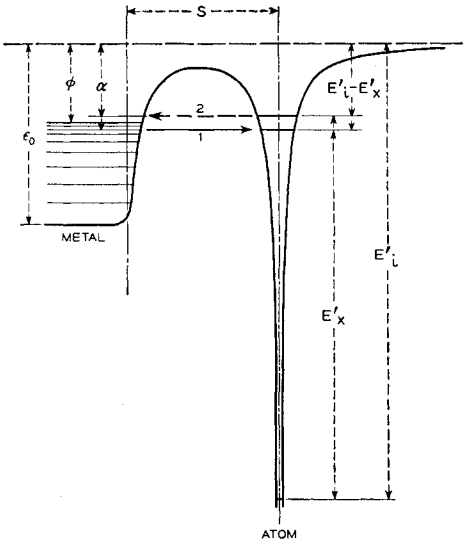

FIG. 1. Schematic diagram illustrating resonance neutralization of an ion (transition 1) or resonance ionization of an excited atom (transition 2) at a metal surface. Transition 1 can occur only at energy levels which are filled inside the metal, transition 2 at levels which are empty. It is evident that for the noble gases resonance ionization of an atom can occur only if the atom is excited. The possibility of shift of a given excited level with distance s such that $(E_i'-E_x')>\varphi$ for $s>s_c$ and $(E_i'-E_x')<\varphi$ for $s>s_c$ is discussed in Sec. X of the text. Notation used is defined in Table I.

[8] W. Ploch, Z. Physik **130**, 174 (1951).
[9] A. Becker, Ann. Physik **75**, 217 (1924).
[10] G. Schneider, Ann. Physik **11**, 357 (1931).
[11] P. L. Kapitza, Phil. Mag. **45**, 989 (1923).
[12] N. D. Morgulis, J. Exptl. Theoret. Phys. (U.S.S.R.) **4**, 449 (1934); **9**, 1484 (1939); **11**, 300 (1941).
[13] S. V. Izmailov, J. Exptl. Theoret. Phys. (U.S.S.R.) **9**, 1473 (1939).
[14] M. E. Gurtovoy, J. Exptl. Theoret. Phys. (U.S.S.R) **10**, 483 (1940).

TABLE I. Definitions of notation.[a]

e^-	electron (subscript M indicates electron is inside metal; energy of electron may be given in parentheses behind the symbol)
X	normal atom
X^m	metastable atom (in some cases any excited atom)
X^+	ion
α, β	energy below the vacuum level of an electron in the metal
$\epsilon, \epsilon', \epsilon''$	energy of an electron in the conduction band measured from the bottom of the band
ϵ_k	energy above bottom of conduction band of excited electron inside metal
$\epsilon_0, \epsilon_0(M)$	energy of vacuum level above bottom of conduction band in metal M
$\epsilon_F, \epsilon_F(M)$	energy of Fermi level of metal M above bottom of conduction band
$\varphi, \varphi(M)$	work function of metal M
E_k	kinetic energy of a particle (ion, atom, electron) outside metal
E_i	ionization energy
E_x	excitation energy
E_i', E_x'	effective ionization and excitation energies near a metal surface, respectively
$E(n-M)$	energy of interaction of normal atom and metal surface
$E(m-M)$	energy of interaction of metastable (sometimes excited) atom and metal surface
$E(i-M)$	energy of interaction of ion and metal surface
E_t	total energy in a system
$\delta(\epsilon)$	Dirac δ function on energy
s	distance of particle from metal surface ($s=0$ at plane of nuclei of surface atoms)
s_c	critical distance for resonance processes: neutralization at $s>s_c$, ionization at $s<s_c$
s_m	distance at which $P_t(s,v_0)$ function is maximum
$\bar{s}$	mean distance at which process occurs
d	particle diameter (subscripts n, m, and i indicate normal atom, metastable atom, and ion, respectively)
v_0	incident velocity of particle toward metal
θ	angle between surface normal and velocity vector of excited electron
θ_c	maximum θ for escape over surface potential barrier
φ	azimuthal angle about surface normal
H_{fi}	matrix element of Auger transition[b]
f	ratio of matrix element for $\theta<\theta_c$ to that for $\theta>\theta_c$[b]
$F(\epsilon',\epsilon'')$	function giving dependence of H_{fi} on initial state energies[b]
$u_M'(1), u_M''(2)$	wave functions of electrons 1 and 2 at ϵ' and ϵ'' in the filled portion of the conduction band, respectively
u_F	wave function of the excited electron at ϵ_k
u_G	wave function of electron in the ground state of the neutralized atom
u_E	wave function of the excited (metastable) electron in the atom
γ_N	electron yield from pure Auger neutralization in electrons per incident particle
γ_D	electron yield from pure Auger de-excitation in electrons per incident particle
γ_i	electron yield per incident particle which is an ion at $s=\infty$
γ_m	electron yield per incident particle which is a metastable atom at $s=\infty$
f_N	fraction of incident ions which decay finally by Auger neutralization
α	atomic polarizability (subscripts n and m indicate normal and metastable atom, respectively)
k_m	wave number of fastest electron in conduction band of metal
A, a	parameters in transition rate function $A\exp(-as)$[b,c]
B, b	parameters in repulsive interaction term $B\exp(-bs)$ (subscripts i, m, n denote ion, metastable atom, and normal atom, respectively)
n	number of electrons inside metal
$W(P_t), W(\Phi_\sigma)$	widths at half-maximum of P_t and Φ_σ functions, respectively
$R_t(s)$	total transition rate[b,c]
$P_\Omega(\theta,\epsilon_k)d\Omega$	probability that an excited electron of energy ϵ_k has its velocity vector lying in $d\Omega=\sin\theta d\theta d\varphi$ at θ, φ[b]
$P_k(\epsilon_k,s)d\epsilon_k$	probability that a process occurring with incident particle at s will produce an excited electron having energy in $d\epsilon_k$ at ϵ_k[b]
$P_t(s,v_0)ds$	probability that a particle starting from $s=\infty$ toward the metal with velocity v_0 will undergo an electronic transition in ds at s[b,c]
$P_0(s,v_0)$	probability that a particle approaching a metal surface with velocity v_0 will reach the distance s without undergoing a specific electronic transition
$P_e(\epsilon_k), P_e(E_k)$	probability that an excited electron of energy $\epsilon_k=E_k+\epsilon_0$ will escape from the metal[b]
$\rho(E_t)$	density of final states in Auger process at total energy E_t
$N_c(\epsilon)$	density of states in conduction band
$N(\epsilon_k)$	density of final states available to excited electrons
$N_i(\epsilon_k)$	distribution in energy of excited electrons inside metal[b]
$N_0(E_k)$	distribution in energy of external secondary electrons[b]
$T(\epsilon)$	Auger transform of $N_c(\epsilon)$ [Eq. (15)][b]
$T_\sigma(\epsilon)$	Auger transform broadened by variation of energy levels and Heisenberg uncertainty principle [Eq. (76)][b]
$I(\delta,s)$	distribution in energy difference δ from the nominal ϵ_k for the elemental Auger process ["line profile," Eq. (74)]
$\Phi_\sigma(y)$	Gaussian distribution [Eq. (80)]
σ	parameter determining spread of Gaussian distribution[b] $[\sigma=(\sigma_1^2+\sigma_2^2)^{\frac{1}{2}}]$
σ_1	σ factor from variation of energy levels[b]
σ_2	σ factor from Heisenberg uncertainty principle[b]

[a] Notation used at only one point in the paper is not included in this table.
[b] No superscript indicates that the quantity refers to Auger neutralization or all processes generally; the superscript prime (') indicates that the quantity refers to Auger de-excitation.
[c] The double-prime superscript (") indicates that the quantity refers to a resonance process.

For slow ions only a negligible amount of kinetic energy can be transferred to an essentially free electron. Furthermore, the theory of thermal emission does not account for the observed dependence of kinetic ejection on work function[15] nor the dependence on ion mass of kinetic ejection by isotopic ions.[8] It appears that the release of bound electrons from surface atoms is the most probable kinetic ejection process for an ion of kinetic energy less than 1000 ev. In the experimental work[7] there is evidence of electrons from kinetic ejection only in the case of He^+ at energies above 400 ev.

[15] H. Paetow and W. Walcher, Z. Physik **110**, 69 (1938).

Kinetic energy may be lost at the metal surface to elastic vibrations in the solid and to sputtered atoms, and in producing disorder in the lattice.[16] It is clear that appreciable kinetic energy loss can occur only at distances from the surface where the repulsive forces are large. Evidence presented in this paper indicates that for slow ions (<100 ev) incident upon atomically clean metal surfaces the Auger processes occur with high probability on the inward trip of the particle toward the surface before processes involving the kinetic energy become important. Consistent with this is the observation of very few reflected ions or metastable atoms (~0.1 percent) for ions of energy less than 100 ev.[7]

Before proceeding with the theory the assumptions made as to the nature of the metal surface will be stated. It is assumed that the surface is smooth and structureless. Thus a one-dimensional theory is given in which no distinction is made between approach directly above a surface atom or between surface atoms. The properties attributed to this surface are those of the polycrystalline surfaces with which the experimental work has been performed.

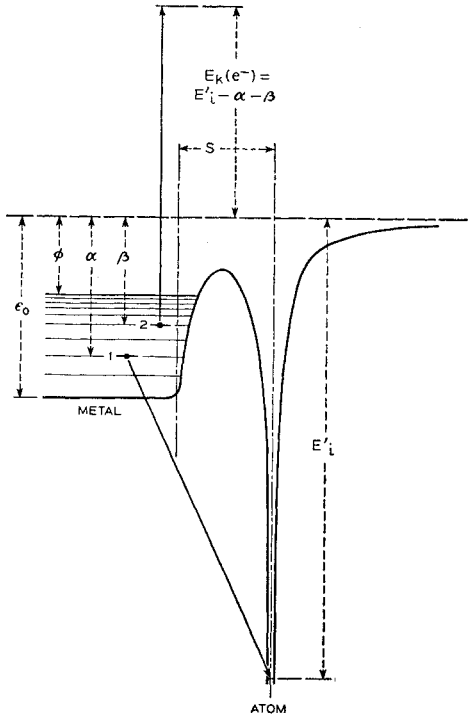

FIG. 2. Schematic diagram illustrating Auger neutralization of an ion at a metal surface. If the excited electron escapes, $E_k(e^-)$ is its kinetic energy observed outside the metal. The limits of $E_k(e^-)$ are seen to be $E_k(e^-)_{max}=E_i'-2\varphi$; $E_k(e^-)_{min}=E_i'-2\epsilon_0$ (zero if $E_i'<2\epsilon_0$). Note that $E_i'>2\varphi$ is necessary for production of an *external* secondary electron. Neutralization by this process can always occur if $E_i'>\varphi$ although resonance neutralization (Fig. 1) is more probable at a given s if $\varphi<E_i'<\epsilon_0$.

[16] See the review of experiment and theory concerning these topics in H. S. W. Massey and E. H. S. Burhop, *Electronic and Ionic Impact Phenomena* (Oxford University Press, London, 1952), pp. 610 ff. and 578 ff. G. K. Wehner, Phys. Rev. **93**, 633 (1954), has recently reported work in which the kinetic energy threshold of sputtering for Hg^+ on tungsten is found to be 80–100 ev.

III. THEORY OF AUGER NEUTRALIZATION

We discuss first the process of Auger neutralization depicted in Fig. 2. For convenience we redraw the energy level diagram (Fig. 4) and measure internal energy, ϵ, from the ground state in the conduction band. Thus

$$\epsilon' = \epsilon_0 - \alpha, \tag{1}$$

$$\epsilon'' = \epsilon_0 - \beta, \tag{2}$$

$$\epsilon_k = \epsilon_0 + E_k. \tag{3}$$

The elemental process of Auger neutralization, with the interacting electrons initially at ϵ' and ϵ'' in the conduction band, consists of the system $X^+ + e_M^-(\epsilon') + e_M^-(\epsilon'')$ transforming itself at constant total energy E_t, into the isoelectronic system $X + e^-(\epsilon_k)$. This transition, which takes place with the atomic particle a

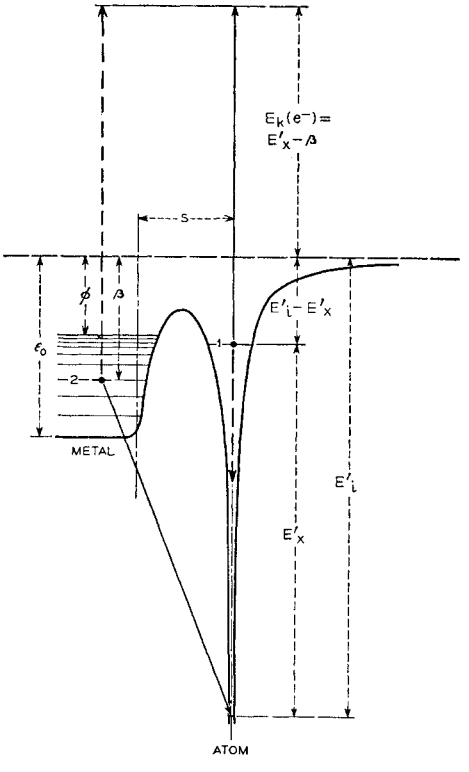

FIG. 3. Schematic diagram illustrating Auger de-excitation of an excited atom at a metal surface. The exchange transition is indicated by the full lines, the process not involving electron exchange between metal and atom by the dashed lines. Note here that the process can occur whenever $E_i'>\varphi$, but that resonance ionization (Fig. 1) followed by Auger neutralization (Fig. 2) is more probable at a given s if $(E_i'-E_x')<\varphi$. External secondary electrons are produced if $E_x'>\varphi$. The kinetic energy extrema are $E_k(e^-)_{max}=E_x'-\varphi$; $E_k(e^-)_{min}=E_x'-\epsilon_0$ (zero if $E_x'<\epsilon_0$).

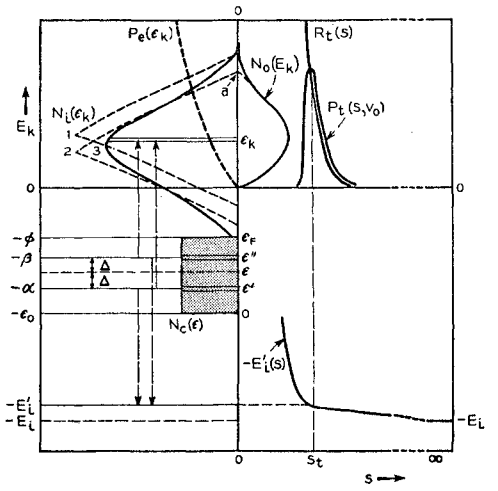

FIG. 4. A composite plot of energy levels, energy distribution functions, and other functional dependences related to the process of Auger neutralization of an ion at a metal surface. The horizontal line labeled 0–0 is the zero energy level in the vacuum. The vertical line labeled 0–0 represents the metal surface. The interior of the metal is at the left, the vacuum outside the metal at the right. The filled portion of the conduction band is indicated between $\epsilon=0$ and $\epsilon=\epsilon_F$ by stippling. The electronic transitions of an elemental Auger neutralization process which populate the energy element $d\epsilon_k$ at ϵ_k are shown as vertical dashed lines. Curve 1 for $N_i(\epsilon_k)$ is obtained if $E_i'=E_i$ and broadening is neglected, curve 2 if $E_i'=E_i'(s_m)$ and broadening neglected, curve 3 if E_i' varies with s as indicated and account is taken of broadening. The $N_0(E_k)$ function shown is that obtained from curve 3 for $N_i(\epsilon_k)$.

distance s from the metal surface, may thus be written

$$X^+ + e_M^-(\epsilon') + e_M^-(\epsilon'') \rightarrow X + e^-(\epsilon_k). \quad (4)$$

The ejection process, of course, must involve the final escape of at least some of the excited electrons $e^-(\epsilon_k)$ from the metal.

If we take the zero of total energy, $E_t=0$, as the energy of the final state $X+e^-$ with both particles at rest an infinite distance from the metal, the energy of the final state in (4) is $E(n-M)+(\epsilon_k-\epsilon_0)$, that of the initial state is $E(i-M)+E_i-(\epsilon_0-\epsilon')-(\epsilon_0-\epsilon'')$. Here $E(n-M)$ and $E(i-M)$ are the energies of interaction of the normal atom and the ion, respectively, with the metal at the distance s from the surface. Equating the energies of the initial and final states, which are each equal to E_t, leads to the relations

$$\epsilon'+\epsilon''=2\epsilon=\epsilon_k+\epsilon_0-E_i'(s), \quad (5)$$

$$E_i'(s)=E_i+E(i-M)-E(n-M). \quad (6)$$

$E'(s)$ defines an effective ionization energy for the atom at a distance s from the metal surface. It should be noted that evaluation of the initial and final energies at the same value of s is the tantamount to assuming that the Franck-Condon principle holds for these electronic transitions. (See Secs. IX and X.)

The transition rate for the process which occurs when the ion is at s, which involves electrons initially at ϵ' and ϵ'' in the metal, and which results in an excited electron of energy ϵ_k with velocity vector lying in the element of solid angle $d\Omega$, is given by the method of variation of constants as

$$(2\pi/\hbar)|H_{fi}|^2\rho(E_t)d\Omega. \quad (7)$$

Here $\rho(E_t)$ is the density of final states at total energy E_t and H_{fi} is the matrix element,[17]

$$H_{fi}=\int\int u_F^*(1)u_G^*(2)(e^2/r_{12})u_M'(1)u_M''(2)d\tau_1 d\tau_2. \quad (8)$$

In (8) u_F is the wave function of the excited electron, u_G is that of the electron in the ground state of the neutralized atom, and the u_M functions are those of electrons in the conduction band in the metal. The perturbation is the Coulomb interaction between the participating electrons. We note that there are, in fact, two processes (4) at energy E_t corresponding to the two possible identifications of the participating electrons on each side of the equation (see Fig. 4). This should be accounted for by antisymmetrizing the wave functions. For the purposes of this paper, in which matrix elements are not calculated, discussion of the characteristics of the matrix element for Auger neutralization is done in terms of the unsymmetrized form (8).

We now write the transition rate (7) for the elemental process in the form

$$(2\pi/\hbar)|H_{fi}|^2N(\epsilon_k)d\Omega=F(\epsilon',\epsilon'')N(\epsilon_k)P_\Omega(\theta,\epsilon_k)d\Omega. \quad (9)$$

In this expression $\rho(E_t)$ has been replaced by the density of final states, $N(\epsilon_k)$, available to the excited electron at ϵ_k inside the metal. $P_\Omega(\theta,\epsilon_k)d\Omega$ is the probability that the excited electron of energy ϵ_k has its velocity vector lying in $d\Omega=\sin\theta d\theta d\varphi$ at the polar angles θ, φ. $F(\epsilon',\epsilon'')$ is a function of initial state energies only. The matrix element is thus assumed to depend only on the angle θ

TABLE II. Table of energies in ev.

Tungsten: $\varphi=4.5$;[a] $\epsilon_F=6.4$;[b] $\epsilon_0=10.9$					
Atom	E_i [c]	E_x [c]	E_i-E_x	$E_i-2\varphi$	$E_x-\varphi$
He	24.58	19.81	4.77	15.58	15.31
Ne	21.56	16.61	4.95	12.56	12.11
Ar	15.76	11.55	4.21	6.76	7.05
Kr	14.00	9.91	4.09	5.00	5.41
Xe	12.13	8.31	3.82	3.13	3.81

[a] See compilation of work function data by H. B. Michaelson, J. Appl. Phys. 21, 536 (1950).
[b] This is Manning and Chodorow's value (reference 24). See discussion in Sec. XVI.
[c] He, Ne, Ar: C. E. Moore, *Atomic Energy Levels*, National Bureau of Standards Circular No. 467 (U. S. Government Printing Office, Washington, D. C., 1949), Vol. I; Kr: National Bureau of Standards Circular No. 467, Vol. II (1952); Xe: Landol-Börnstein, *Tables* (Julius Springer, Berlin, 1950), Vol. 1, Part 1.

[17] Matrix elements for the Auger effect are discussed in E. H. S. Burhop, *The Auger Effect and Other Radiationless Transitions* (Cambridge University Press, London, 1952), Chap. II, Secs. 2.1 and 2.4. See also reference 3.

with the surface normal and to be independent of aximuthal angle φ.

The total transition rate for all processes occurring when the ion is at a distance s from the surface is

$$R_t(s)=\int\int\int\int(2\pi/\hbar)|H_{fi}|^2N(\epsilon_k)d\Omega d\epsilon_k \times\delta(\epsilon'+\epsilon''+E_i'-\epsilon_0-\epsilon_k)N_c(\epsilon')N_c(\epsilon'')d\epsilon'd\epsilon'', \quad (10)$$

which, by use of (9), may be written

$$R_t(s)=\int\int N(\epsilon_k)P_\Omega(\theta,\epsilon_k)\int\int F(\epsilon',\epsilon'') \times\delta(\epsilon'+\epsilon''+E_i'-\epsilon_0-\epsilon_k)N_c(\epsilon') \times N_c(\epsilon'')d\epsilon'd\epsilon''d\Omega d\epsilon_k. \quad (11)$$

In (10) and (11) $N_c(\epsilon)$ is the state density function in the conduction band. The Dirac δ function on energy assures compliance with the energy condition (5).

The function $F(\epsilon',\epsilon'')$ expresses the unknown dependence of H_{fi} on the initial state energies. We may proceed by assuming either that $F(\epsilon',\epsilon'')$ is a constant or that the effect of $F(\epsilon',\epsilon'')$ in the integral over ϵ' and ϵ'' in (11) may be approximated by the use of an effective state density function $N_c(\epsilon)$. Then

$$R_t(s)=C\int\int N(\epsilon_k)P_\Omega(\theta,\epsilon_k)\int\int\delta(\epsilon'+\epsilon''+E_i'-\epsilon_0-\epsilon_k) \times N_c(\epsilon')N_c(\epsilon'')d\epsilon'd\epsilon''d\Omega d\epsilon_k, \quad (12)$$

in which C is a constant.

If we now make the change of variable,

$$\epsilon'=\epsilon-\Delta, \quad \epsilon''=\epsilon+\Delta, \quad (13)$$

indicated in Fig. 4, and specify limits, the double integral in (12) becomes

$$\int_0^{\epsilon_F/2}\int_0^{\epsilon}N_c(\epsilon-\Delta)N_c(\epsilon+\Delta)\delta(2\epsilon+E_i'-\epsilon_0-\epsilon_k)d\Delta d\epsilon + \int_{\epsilon_F/2}^{\epsilon_F}\int_0^{\epsilon_F-\epsilon}N_c(\epsilon-\Delta)N_c(\epsilon+\Delta) \times\delta(2\epsilon+E_i'-\epsilon_0-\epsilon_k)d\Delta d\epsilon = \int_0^{\epsilon_F}T(\epsilon)\delta(2\epsilon+E_i'-\epsilon_0-\epsilon_k)d\epsilon = T[(\epsilon_k+\epsilon_0-E_i')/2]. \quad (14)$$

Here $T(\epsilon)$ is the so-called Auger transform[18] defined thus:

$$T(\epsilon)=\int_0^{\epsilon}N_c(\epsilon-\Delta)N_c(\epsilon+\Delta)d\Delta, \quad 0<\epsilon<\epsilon_F/2$$
$$=\int_0^{\epsilon_F-\epsilon}N_c(\epsilon-\Delta)N_c(\epsilon+\Delta)d\Delta, \quad \epsilon_F/2<\epsilon<\epsilon_F$$
$$=0; \quad \epsilon<0, \quad \epsilon>\epsilon_F. \quad (15)$$

The total transition rate, from (12) and (14), is thus:

$$R_t(s)=C\int\int N(\epsilon_k)T[(\epsilon_k+\epsilon_0-E_i')/2]P_\Omega(\theta,\epsilon_k)d\Omega d\epsilon_k =C\int_{\epsilon_F}^{\infty}N(\epsilon_k)T[(\epsilon_k+\epsilon_0-E_i')/2]d\epsilon_k, \quad (16)$$

since $\int_0^{2\pi}\int_0^{\pi}P_\Omega(\theta,\epsilon_k)\sin\theta d\theta d\varphi=1$ at all ϵ_k. In (16) account is taken of the fact that only states for which $\epsilon_k>\epsilon_F$ are available as final states inside the metal. We neglect the small population of states above ϵ_F demanded by the Fermi distribution at temperatures above absolute zero.

We now define a second probability distribution function $P_k(\epsilon_k,s)$ such that $P_k(\epsilon_k,s)d\epsilon_k$ is the probability that the excited electron produced in a process occurring with the ion at s will have energy in the interval $d\epsilon_k$ at ϵ_k. Then $R_t(s)$ may be written as

$$R_t(s)=\int\int R_t(s)P_k(\epsilon_k,s)P_\Omega(\theta,\epsilon_k)d\Omega d\epsilon_k =\int_{\epsilon_F}^{\infty}R_t(s)P_k(\epsilon_k,s)d\epsilon_k, \quad (17)$$

from which, with (16),

$$P_k(\epsilon_k,s)=\frac{N(\epsilon_k)T[(\epsilon_k+\epsilon_0-E_i')/2]}{\int_{\epsilon_F}^{\infty}N(\epsilon_k)T[(\epsilon_k+\epsilon_0-E_i')/2]d\epsilon_k}, \quad \epsilon_k>\epsilon_F$$
$$=0, \quad \epsilon_k<\epsilon_F. \quad (18)$$

The dependence of P_k on s comes through the dependence of E_i' on s [Eq. (6)].

We wish now to determine the distribution in energy, $N_i(\epsilon_k)$, of electrons excited in the Auger neutralization process. To do this we need the probability $P_t(s,v_0)ds$ that an incoming ion of velocity v_0, assumed constant, undergoes Auger neutralization in the distance interval ds at s. $P_t(s,v_0)$ is determined from $R_t(s)$ in Sec. V. Illustrative R_t and P_t functions are plotted in Fig. 4. Using the probability distributions P_k and P_Ω defined

[18] The author first encountered this Auger transform in the work of J. J. Lander, (private communication) Phys. Rev. 91, 1382 (1953), to whom he is much indebted.

previously, we may write

$$N_i(\epsilon_k)=\int_0^\infty\int_0^{2\pi}\int_0^{\pi} P_t(s,v_0)P_k(\epsilon_k,s) \times P_\Omega(\theta,\epsilon_k)\sin\theta d\theta d\varphi ds$$
$$=\int_0^\infty P_t(s,v_0)P_k(\epsilon_k,s)ds. \quad (19)$$

In writing this expression it has been assumed that all significant contributions to $N_i(\epsilon_k)$ occur on the inward trip of the ion toward the metal surface. The justification for this in the light of the experimental evidence is discussed in Sec. XIII. The integral of $N_i(\epsilon_k)$ over all ϵ_k is thus

$$\int_0^\infty N_i(\epsilon_k)d\epsilon_k=\int_0^\infty P_t(s,v_0)ds\simeq 1, \quad (20)$$

since $\int_0^\infty P_k(\epsilon_k,s)d\epsilon_k=1$ at all s. $N_i(\epsilon_k)$ is thus normalized to a total area of one electron per incident ion when Auger neutralization is the only possible Auger process.

Even with $\int_0^\infty P_t(s,v_0)ds=1$ one cannot determine $N_i(\epsilon_k)$ without integration over s because $P_k(\epsilon_k,s)$ depends on s. A method of approximating the integration over s in Eq. (19) is suggested by the fact that $P_t(s,v_0)$ is large over only a relatively small range of s. The effect of $P_t(s,v_0)$ in (19) is thus to broaden somewhat the function $P_k(\epsilon_k,s)$ evaluated at the distance $s=s_m$ at which $P_t(s,v_0)$ is a maximum. The results of this procedure are discussed in Secs. XII and XIV. If the interaction energies $E(n-M)$ and $E(i-M)$ in (6) are neglected, $E_i'(s)=E_i$, a constant, P_k becomes independent of s and $N_i(\epsilon_k)=P_k(\epsilon_k)$ if $\int_0^\infty P_t(s,v_0)ds$ is taken to be unity. The consequences of these assumptions are discussed in Sec. VII.

The distribution in energy, $N_0(\epsilon_k)$, of electrons which escape from the metal is

$$N_0(\epsilon_k)=\int_0^\infty\int_0^{2\pi}\int_0^{\theta_c} P_t(s,v_0)P_k(\epsilon_k,s) \times P_\Omega(\theta,\epsilon_k)\sin\theta d\theta d\varphi ds$$
$$=\int_0^\infty P_t(s,v_0)P_k(\epsilon_k,s)ds \times\int_0^{2\pi}\int_0^{\theta_c} P_\Omega(\theta,\epsilon_k)\sin\theta d\theta d\varphi$$
$$=N_i(\epsilon_k)P_e(\epsilon_k). \quad (21)$$

Here $\theta_c(\epsilon_k)$ is the maximum value of θ for which escape of the excited electron over the surface barrier is possible. The quantity $P_e(\epsilon_k)$, defined by the equation

$$P_e(\epsilon_k)=\int_0^{2\pi}\int_0^{\theta_c} P_\Omega(\theta,\epsilon_k)\sin\theta d\theta d\varphi, \quad (22)$$

is the probability that an excited electron of energy ϵ_k will escape over the surface barrier. It is discussed further in Sec. VI. Since $P_e(\epsilon_k)>0$ only if $\epsilon_k>\epsilon_0$ (or $E_k>0$) we shall usually write N_0 as a function of $E_k=\epsilon_k-\epsilon_0$. Illustrative $N_i(\epsilon_k)$, $P_e(\epsilon_k)$, and $N_0(E_k)$ functions are shown in Fig. 4.

Finally we obtain the total electron yield, γ_N, in electrons per incident particle for the process of Auger neutralization by integrating $N_0(E_k)$ over E_k. Thus,

$$\gamma_N=\int_0^\infty N_0(E_k)dE_k. \quad (23)$$

This is one of four secondary electron yield parameters which are introduced in this paper. γ_N defined above and γ_D to be defined similarly in the next section are the yields for the so-called pure Auger neutralization and de-excitation processes, respectively, that is, for processes in which all incident particles decay by the process in question. These yields are clearly to be distinguished from γ_i and γ_m which are the experimentally observed yields for incident ions and metastable atoms, respectively. Thus, for example, we cannot identify γ_i with γ_N until it has been demonstrated that each incident ion finally decays to the ground state of the atom via Auger neutralization. The possibility exists that in some cases a fraction of the ions will be resonance neutralized and that the excited atoms so formed will undergo Auger de-excitation. The total observed yield per incident ion, γ_i, must then be compounded by γ_N and γ_D as described in Sec. XIV.

IV. THEORY OF AUGER DE-EXCITATION

We turn now to a discussion of Auger de-excitation of a metastable atom at a metal surface (Fig. 3).[19] The process which proceeds at constant total energy E_t may be written

$$X^m+e_M^-(\epsilon'')\rightarrow X+e^-(\epsilon_k), \quad (24)$$

where $\epsilon''=\epsilon_0-\beta$, it being understood that only a fraction of the excited electrons $e^-(\epsilon_k)$ leave the metal. Again taking E^t to be zero for X and e^- at rest an infinite distance from the metal we find that $E_t=E_x+E(m-M)-(\epsilon_0-\epsilon'')=(\epsilon_k-\epsilon_0)+E(n-M)$, from which

$$\epsilon''=\epsilon_k-E_x'(s), \quad (25)$$

$$E_x'(s)=E_x+E(m-M)-E(n-M). \quad (26)$$

Here $E(m-M)$ and $E(n-M)$ are the interaction energies of the metastable atom and the normal atom with the metal surface, respectively. $E_x'(s)$ defines an effective excitation energy for the atom at a distance s from the metal surface. Again the Franck-Condon principle is assumed in evaluating the energies which depend on s.

The formalism developed above for Auger neutralization may be taken over for Auger de-excitation if it

[19] Even though the discussion and notation refer here to metastable atoms it is clear that any excited atom near the metal may undergo Auger de-excitation.

is assumed that ϵ' is a constant at the value demanded by resonance capture of the first electron into the isoenergetic excited level in the atom. Thus,

$$\epsilon' = \epsilon_0 - \alpha = \epsilon_0 - (E_i' - E_x'), \tag{27}$$

$$E_i' - E_x' = (E_i - E_x) + E(i-M) - E(m-M), \tag{28}$$

from Eqs. (1), (6), and (26).

The transition rate for the process at constant E_t again has the form of relation (7) above with $\rho(E_t)$ again equal to $N(\epsilon_k)$. The matrix element, H_{fi}', for Auger de-excitation may be written as follows for processes in which an electron is or is not exchanged between metal and atom, respectively:

$$(H_{fi}')_{\text{exch}} = \int\int u_F^*(1) u_G^*(2) (e^2/r_{12}) \times u_E(1) u_M''(2) d\tau_1 d\tau_2, \tag{29}$$

$$(H_{fi}')_{\text{nonexch}} = \int\int u_F^*(2) u_G^*(1) (e^2/r_{12}) \times u_E(1) u_M''(2) d\tau_1 d2_2. \tag{30}$$

Here the u_E function, not previously defined, is the wave function of the electron in the excited (metastable) state in the atom. Both matrix elements are written out here for use in subsequent discussion.

The transition rate for the elemental Auger de-excitation process, in analogy to (9), is written in the form $F'(\epsilon'')N(\epsilon_k)P_\Omega'(\theta,\epsilon_k)d\Omega$, and the total transition rate for all processes occurring at s as

$$R_t'(s) = \int\int N(\epsilon_k) P_\Omega'(\theta,\epsilon_k) \int F'(\epsilon'') \times \delta(\epsilon'' + E_x' - \epsilon_k) N_c(\epsilon'') d\epsilon'' d\Omega d\epsilon_k. \tag{31}$$

The primed functions F', P_Ω', R_t' and the functions T', P_k', N_i', N_0', and P_e' to be introduced presently have the same definitions with respect to Auger de-excitation as do the unprimed functions for Auger neutralization. If F' is assumed constant (C') or its dependence on ϵ'' included in an effective $N_c(\epsilon'')$ function, the transition rate is

$$R_t'(s) = C' \int_{\epsilon_F}^{\infty} N(\epsilon_k) N_c(\epsilon_k - E_x') d\epsilon_k = C' \int_{\epsilon_F}^{\infty} N(\epsilon_k) T'(\epsilon_k - E_x') d\epsilon_k. \tag{32}$$

Thus the Auger transform for the de-excitation process is the state density function (or an effective one including the possible dependence of the matrix element on ϵ''). Thus,

$$T'(\epsilon) = N_c(\epsilon). \tag{33}$$

It follows that other functions describing Auger de-excitation are

$$P_k'(\epsilon_k, s) = \frac{N(\epsilon_k) N_c(\epsilon_k - E_x')}{\int_{\epsilon_F}^{\infty} N(\epsilon_k) N_c(\epsilon_k - E_x') d\epsilon_k}, \quad \epsilon_k > \epsilon_F = 0, \quad \epsilon_k < \epsilon_F \tag{34}$$

and $N_{ii}(\epsilon_k)$, $N_{0i}(\epsilon_k)$, and $P_{ei}(\epsilon_k)$, which are identical in form with the corresponding functions for Auger neutralization defined in Eqs. (19), (21), and (22), respectively. If Auger de-excitation is the only process possible the total yield of secondary electrons per incident particle, which we call γ_D, is the integral of $N_0'(E_k)$ over E_k in analogy to the definition of γ_N in Eq. (23).

V. TRANSITION RATE AND RELATED PROBABILITY FUNCTIONS

The characteristics of the matrix elements for the Auger processes are specified by the functions R_t, P_Ω, and F. The total transition rate, $R_t(s)$, specifies the dependence of the matrix element on s; $P_\Omega(\theta,\epsilon_k)$ gives the dependence on angle which the excited electron's velocity vector makes with the surface normal; $F(\epsilon',\epsilon'')$ accounts for the dependence on initial state energies. F has been assumed a constant or its effect considered to be accounted for by use of an effective state density function, $N_c(\epsilon)$. The functions R_t and P_Ω are discussed in this section and the next, respectively.

Upon specific evaluation of matrix elements both Shekhter[3] [his Eq. (3.11)] and Cobas and Lamb[4] [their Eq. (5)] find $R_t(s)$ to be expressed as an exponential in s multiplied by a polynomial in s. In view of the fact that each of the processes being considered occurs over a limited range of s only it is sufficient to assume

$$R_t(s) = A \exp(-as). \tag{35}$$

The form (35) is taken to be appropriate for Auger neutralization (A,a), exchange de-excitation (A',a'), and the resonance processes (A'',a'').

The matrix element for the nonexchange Auger de-excitation [Eq. (30)] is zero if the states u_E and u_G have different spins and is small if u_E and u_G are both S states. In other cases the matrix element may be expected to vary algebraically with s. Since we shall assume the rate functions for Auger neutralization and de-excitation to be equal ($A = A'$, $a = a'$) we are in effect neglecting the nonexchange de-excitation process. Note the similarities between the matrix elements for Auger neutralization and exchange de-excitation [Eqs. (8) and (29), respectively]. It is possible to estimate a value for a with reasonable accuracy. The parameter A is determined by fitting the theory to the experimental results as discussed in Sec. XIII.

In the matrix elements (8) and (29) exponential terms involving s arise in the $u_G^*(2)$ and $u_M''(2)$

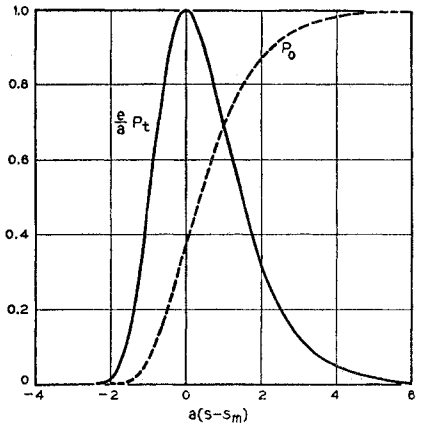

FIG. 5. Plots of the P_0 and P_t functions given in Eqs. (43) and (44) in the text. P_0 is the probability that an incident particle subject to a single electronic transition process, will reach s without the process occurring. P_t is the probability distribution governing transition in ds at s. s_m is defined by Eq. (40) and the transition rate function $R_t(s)$ by Eq. (35).

functions. These terms are of the form $\exp(-\lambda s)$ with $\lambda=(2m\eta/\hbar^2)^{\frac{1}{2}}$. For the atomic function $\eta=E_i$; for the metal function η lies in range $\varphi<\eta<\epsilon_0$. We thus expect that at large distances the exponential from the metal function will predominate. A value of $a=2\lambda$ of the order of 3×10^8 cm^{-1} is estimated in this way. Values of a which arise in the matrix element calculation are listed in Table X. Cobas and Lamb's value for a' may perhaps be expected to be somewhat large because the wave functions for the metallic electrons were taken to be zero outside the metal. Calculations have been carried out in the present work with the values $a=2\times10^8$ cm^{-1} and 5×10^8 cm^{-1}. It will be seen that these values represent limits between which the value of a for Auger neutralization most likely lies (see Sec. XIII). Very little of a quantitative nature comes out of the present work concerning the parameters A'' and a'' for the resonance process.

If we start with the transition rate, $R_t(s)$, it is convenient to derive two related probability functions. From the definition of $R_t(s)$ it follows that $R_t(s)ds/v_0$ is the probability that a particle in moving with speed v_0 through the element ds at s will undergo transition. Then the probability $P_0(s,v_0)$ that the incident particle starting from an infinite distance toward the metal will reach the distance s *without* undergoing transition is

$$P_0(s,v_0)=\exp\left[-\int_s^\infty R_t(s)ds/v_0\right]. \tag{36}$$

The probability that the particle, having started from infinity, will undergo transition in ds at s is then

$$P_t(s,v_0)ds=[R_t(s)ds/v_0]\exp\left[-\int_s^\infty R_t(s)ds/v_0\right]. \tag{37}$$

Evidently P_0 and P_t functions may be defined for each of the resonance and Auger processes. Putting the exponential form (35) for $R_t(s)$ into Eqs. (36) and (37) and assuming v_0 to be constant, we obtain

$$P_0(s,v_0)=\exp[-(A/av_0)\exp(-as)] \tag{38}$$

and

$$P_t(s,v_0)=(A/v_0)\exp[-(A/av_0)\exp(-as)-as]. \tag{39}$$

Cobas and Lamb[4] have derived the expressions (37) and (39) for the probability distribution $P_t(s,v_0)$.

The $P_t(s,v_0)$ function may be shown to pass through a maximum value at $s=s_m$ with

$$s_m=(1/a)\ln(A/av_0). \tag{40}$$

The value of $P_t(s,v_0)$ at $s=s_m$ is

$$P_t(s_m)=a/e=0.368a, \tag{41}$$

independent of v_0. A graphical solution gives for the width on the s scale of the P_t function at half-maximum,

$$W(P_t)=2.48/a. \tag{42}$$

Written in terms of s_m expressions (38) and (39) become

$$P_0(s,v_0)=\exp\{-\exp[-a(s-s_m)]\}, \tag{43}$$

and

$$P_t(s,v_0)=a\exp\{-\exp[-a(s-s_m)]-a(s-s_m)\}. \tag{44}$$

These expressions depend upon v_0 only through s_m. Thus the form of each is independent of v_0 but the placement relative to the metal surface is determined by v_0 through Eq. (40). The P_0 and P_t functions of (43) and (44) are plotted in Fig. 5.

It is of interest to calculate the mean distance $\bar{s}$ at which a process occurs where $\bar{s}$ is defined by the integral

$$\bar{s}=\int_0^\infty sP_t(s,v_0)ds. \tag{45}$$

By means of (39) $\bar{s}$ can be shown to be[20]

$$\bar{s}=(1/a)[C+\ln(A/av_0)+E_i(A/av_0)], \tag{46}$$

in which C is Euler's constant $(0.5772\cdots)$ and $E_i(y)$ is the exponential integral $\int_y^\infty \exp(-z)dz/z$. As A/av_0 will turn out to be of the order 10^2 or more, the E_i term is completely negligible. Thus,

$$\bar{s}-s_m=C/a=0.58/a. \tag{47}$$

For $a=2\times10^8$ cm^{-1}, $\bar{s}-s_m$ is of the order of 0.3 A so that without a great deal of error we may use s_m and $\bar{s}$ interchangeably.

If it is assumed that the exponential transition rate of Eq. (35) holds to $s=0$ it can be shown that

$$\int_0^\infty P_t(s,v_0)ds=1-P_0(0,v_0)=1-\exp(-A/av_0)$$
$$=1-\exp[-\exp(as_m)]. \tag{48}$$

[20] The author is much indebted to Miss M. C. Gray for performing this integration.

This integral is of interest because it specifies the probability that the process occurs on the inward trip toward the metal surface. From (48) it follows that

$$\lim_{v_0\to 0}\int_0^\infty P_t(s,v_0)ds=1. \tag{49}$$

For the lower ion velocities used in the experimental work s_m is large enough to make the probability of Auger neutralization on the inward trip very nearly unity (Sec. XIII).

VI. THE PROBABILITY OF ESCAPE OF AN EXCITED ELECTRON FROM THE METAL

The probability that an excited electron of energy ϵ_k will leave the metal is defined by Eq. (22). The critical angle θ_c, which is the maximum value of θ for escape over the surface barrier, is readily calculable. Refraction at the surface is such that

$$\epsilon_k\cos^2\theta=\epsilon_0+(\epsilon_k-\epsilon_0)\cos^2\theta', \tag{50}$$

where θ and θ' are the angles of the electron's velocity vector with the surface normal inside and outside the metal, respectively (Fig. 6). If the electron is to leave the metal it is necessary that $\theta'>0$. If $\theta'=0$, then $\theta=\theta_c$, where

$$\theta_c=\cos^{-1}(\epsilon_0/\epsilon_k)^{\frac{1}{2}}. \tag{51}$$

The probability distribution $P_\Omega(\theta,\epsilon_k)$ can be obtained from first principles only by evaluating H_{fi}. In lieu of this the simplest *a priori* assumption one can make about the angular distribution is that it is isotropic. Then P_Ω is a constant and equal to $1/4\pi$, and

$$\begin{aligned}P_e(\epsilon_k)&=\tfrac{1}{2}[1-(\epsilon_0/\epsilon_k)^{\frac{1}{2}}], \quad \epsilon_k>\epsilon_0\\ &=0, \quad \epsilon_k<\epsilon_0\end{aligned} \tag{52}$$

by Eq. (22).

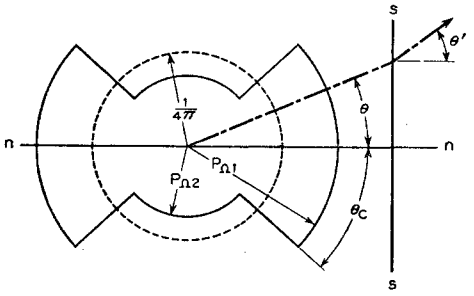

FIG. 6. Polar plot of the probability distribution $P_\Omega(\theta,\epsilon_k)$. The P_Ω surfaces are figures of revolution about the surface normal n–n. The dashed circle represents the isotropic distribution. The full line contour, made up of circles of radii $P_{\Omega 1}$ and $P_{\Omega 2}$, corresponds to a constant matrix element for $\theta<\theta_c$ f times larger than the constant matrix element for $\theta>\theta_c$. This P_Ω surface is symmetrical about the plane through its center parallel to the surface s–s. The specific values of $P_{\Omega 1}$ and $P_{\Omega 2}$ used in this plot are calculated from Eqs. (53) and (54) for $f=2.2$, $\epsilon_0=10.9$ ev, $\epsilon_k=18.9$ ev. Shown also on the figure is the refraction of the path of an electron which approaches the surface s–s at an angle θ and escapes at the angle θ'. $\theta=\theta_c$ is the critical angle for escape at which $\theta'=0$.

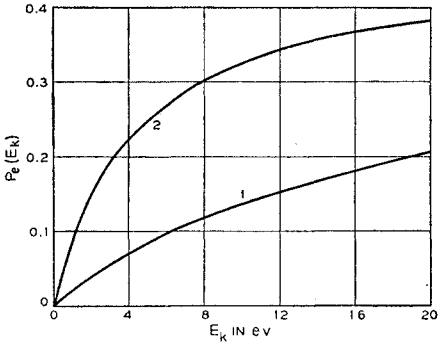

FIG. 7. Plots of two electron escape probability functions $P_e(E_k)$ Curve 1 is that appropriate to an isotropic distribution of electron velocities inside the metal [Eq. (52) in the text]. Curve 2 is a plot of Eq. (55) with $f=2.2$. The parameter f for curve 2 has been chosen so that the theoretical $\gamma_i(\mathrm{He}^+)$ at $E_k(\mathrm{He}^+)=40$ ev equals the experimental value.

Expression (52) for $P_e(\epsilon_k)$ is plotted as curve 1 in Fig. 7. γ_N values calculated with it are found uniformly to be much too small (Table IV). As is pointed out in Sec. VII this can only mean that P_Ω is not isotropic but is of such form as to favor the production of electrons which escape from the metal. Inspection of the matrix elements (8) and (29) shows that this result is in fact to be expected. H_{fi} in (8) may be regarded as the electrostatic interaction energy of two charge clouds of the form $eu_F^*(1)u_M'(1)$ and $eu_G^*(2)u_M''(2)$. Clearly the value of H_{fi} will depend strongly on the value of the first of these clouds near the atomic particle since the second cloud is in some degree localized there by $u_G^*(2)$. It is evident that $eu_F^*(1)u_M'(1)$ will be larger near the atom if u_F represents an electron which can leave the metal than if it represents an electron internally reflected at the surface barrier. C. Herring has suggested to the author that it is reasonable to assume the matrix element constant for $\theta<\theta_c$ and of value (H_1) greater than the value (H_2), also assumed constant, which it has for $\theta>\theta_c$. If $P_{\Omega 1}$ and $P_{\Omega 2}$ are the constant values of $P_\Omega(\theta,\epsilon_k)$ for $\theta<\theta_c$ and $\theta>\theta_c$, respectively, and if $H_1/H_2=f$, it follows that

$$P_{\Omega 1}/P_{\Omega 2}=|H_1/H_2|^2=f^2. \tag{53}$$

The $P_\Omega(\theta,\epsilon_k)$ function, furthermore, should be symmetrical about the origin because $H_{fi}(\theta)=iH_{fi}(\pi+\theta)$. This latter fact follows from the circumstance that in (8) u_M', u_M'', and u_G may be taken as real functions and u_F is of the form $\exp(i\mathbf{k}\cdot\mathbf{r})$.

The $P_\Omega(\theta,\epsilon_k)$ function which we assume is thus of the form shown by the solid curve of Fig. 6. Normalization ($\int\int P_\Omega d\Omega=1$) yields

$$P_{\Omega 1}=(1/4\pi)[1-(1-1/f^2)(\epsilon_0/\epsilon_k)^{\frac{1}{2}}]^{-1}. \tag{54}$$

The resulting $P_e(\epsilon_k)$ function from (22) is

$$\begin{aligned}P_e(\epsilon_k)&=\tfrac{1}{2}\left[\frac{1-(\epsilon_0/\epsilon_k)^{\frac{1}{2}}}{1-(1-1/f^2)(\epsilon_0/\epsilon_k)^{\frac{1}{2}}}\right], \quad \epsilon_k>\epsilon_0\\ &=0, \quad \epsilon_k<\epsilon_0.\end{aligned} \tag{55}$$

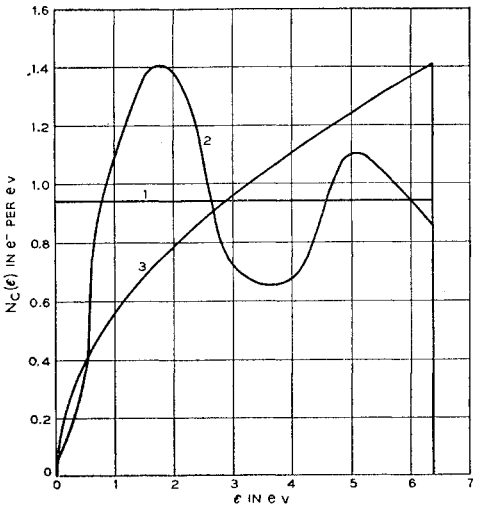

FIG. 8. Plots of three possible state density functions for the conduction band of tungsten. Curve 1. $N_c(\epsilon)=k_1$ (a constant) $=0.94$ electron per ev; 2. The $N_c(\epsilon)$ functions derived by Manning and Chodorow (reference 24); 3. $N_c(\epsilon)=k_2\epsilon^{\frac{1}{2}}=0.555\epsilon^{\frac{1}{2}}$. Each function is normalized to give six valence electrons in the band from $\epsilon=0$ to $\epsilon=\epsilon_F=6.4$ ev.

Expression (55) has been used in the present work.[21] The parameter f has been determined by fitting to the γ_i data for He^+ at 40-ev ions. As discussed in Sec. XIII this gives $f=2.2$, a reasonable value for the ratio of the matrix elements H_1 and H_2. $P_e(\epsilon_k)$ from expression (55) with $f=2.2$, $(1-1/f^2)=0.987$, is plotted as curve 2 in Fig. 7.

In this paper we use the same $P_e(\epsilon_k)$ function for Auger neutralization and de-excitation. That $P_{\Omega 1}/P_{\Omega 2}$ is the same in the two cases appears reasonable because the u_F function appears in the matrix elements (8) and (29) in the same way. Inasmuch as the image barrier extends well beyond the position of the atomic particle we may use the same value of θ_c in either case.

It should be pointed out that in obtaining an expression for $P_e(\epsilon_k)$, we have taken no account of possible changes in direction caused by electron-electron collisions inside the metal. The justification for this neglect lies in the calculations of Wolff[22] which show that an excited electron loses about one-half of its energy per collision and thus quickly sinks back into the Fermi sea.

Finally, it should also be noted that the reflection coefficient at the metal surface for electrons of normal components of energy greater than the barrier height has been assumed zero. That it is small for tungsten in general has been pointed out by Herring and Nichols.[23]

VII. ENERGY DISTRIBUTION AND YIELD NEGLECTING LEVEL SHIFTS AND BROADENING

In this section we shall obtain the form of the electron energy distributions and relative electron yields for the cases of pure Auger neutralization and pure Auger de-excitation neglecting the variation of atomic energy levels near the metal and the effect of the Heisenberg uncertainty principle. Although admittedly crude, these determinations illustrate the basic procedures of the theory and indicate in what ways the theory should be refined. The calculations have been carried out for the singly charged ions and the metastable atoms of lowest energy of each of the noble gasses He, Ne, Ar, Kr, and Xe.

Assumption of no atomic energy level shifts near the metal means that $E_i'=E_i$ and $E_x'=E_x$. The P_k function of Eq. (18) is thus independent of s, and the distribution in energy, $N_i(\epsilon_k)$, of electrons excited in the Auger processes has the form of P_k by (19) and (20). The P_k and P_k' functions in turn are obtained from the assumed initial and final state density functions by Eqs. (18) and (15), and (34), respectively.

TABLE III. Expressions for Auger transforms.[a]

Auger neutralization

$$N_c(\epsilon)=k_1,\ 0<\epsilon<\epsilon_F;\ =0,\ \epsilon>\epsilon_F$$

$$T(\epsilon)=k_1^2\epsilon,\quad 0<\epsilon<\epsilon_F/2$$
$$=k_1^2(\epsilon_F-\epsilon),\quad \epsilon_F/2<\epsilon<\epsilon_F$$

$$T_\sigma(\epsilon)=[k_1^2\sigma/(2\pi)^{\frac{1}{2}}]\{\exp[-\epsilon^2/2\sigma^2]-2\exp[-(\epsilon_F/2-\epsilon)^2/2\sigma^2]+\exp[-(\epsilon_F-\epsilon)^2/2\sigma^2]\}$$
$$+(k_1^2\epsilon/2)\{\mathrm{erf}[\epsilon/\sigma\sqrt{2}]+2\,\mathrm{erf}[(\epsilon_F/2-\epsilon)/\sigma\sqrt{2}]-\mathrm{erf}[(\epsilon_F-\epsilon)/\sigma\sqrt{2}]\}$$
$$+(k_1^2\epsilon_F/2)\{\mathrm{erf}[(\epsilon_F-\epsilon)/\sigma\sqrt{2}]-\mathrm{erf}[(\epsilon_F/2-\epsilon)/\sigma\sqrt{2}]\},$$

$$N_c(\epsilon)=k_2\epsilon^{\frac{1}{2}},\ 0<\epsilon<\epsilon_F;\ =0,\ \epsilon>\epsilon_F$$

$$T(\epsilon)=\pi k_2^2\epsilon^2/4,\quad 0<\epsilon<\epsilon_F/2$$
$$=(k_2^2/2)\{(\epsilon_F-\epsilon)[2\epsilon\epsilon_F-\epsilon_F^2]^{\frac{1}{2}}+\epsilon^2\sin^{-1}[(\epsilon_F-\epsilon)/2]\},\quad \epsilon_F/2<\epsilon<\epsilon_F.$$

Auger de-excitation

$$N_c(\epsilon)=k_1,\ 0<\epsilon<\epsilon_F;\ =0,\ \epsilon>\epsilon_F$$

$$T'(\epsilon)=k_1,$$

$$T_{\sigma'}(\epsilon)=(k_1/2)\{\mathrm{erf}[(\epsilon_F-\epsilon)/\sigma'\sqrt{2}]+\mathrm{erf}[\epsilon/\sigma'\sqrt{2}]\}.$$

[a] These functions are plotted in Figs. 9 and 26 for the specific case of tungsten ($\epsilon_F=6.4$ev; $\int_0^{\epsilon_F}N_c(\epsilon)d\epsilon=6$ electrons).

[21] It is interesting to note that one can derive other one-parameter $P_e(\epsilon_k)$ functions which at one end of the range of the parameter give expression (52) for isotropic P_Ω and at the other end give $P_e(\epsilon_k)=\frac{1}{2}$ independent of ϵ_k. Two such may be obtained by assuming P_Ω to be independent of ϵ_k and proportional to: 1, the area within $d\Omega$ on the surface of an oblate spheroid of eccentricity e, and 2, the volume of the spheroid within $d\Omega$. The first of these assumptions leads to

$$P_e(\epsilon_k)=\tfrac{1}{2}\left[1-\frac{\tanh^{-1}e(\epsilon_0/\epsilon_k)^{\frac{1}{2}}}{\tanh^{-1}e}\right].$$

The second assumption gives

$$P_e(\epsilon_k)=\tfrac{1}{2}\left[1-\left(\frac{(1-e^2)(\epsilon_0/\epsilon_k)}{1-e^2(\epsilon_0/\epsilon_k)}\right)^{\frac{1}{2}}\right].$$

When fitted to $\gamma_i(He^+)$ at 40 ev we get $e=0.984$ for the first expression, $e=0.928$ for the second. Although the $P_e(\epsilon_k)$ functions thus obtained agree quite closely with expression (55) with $f=2.2$, the ratio of P_Ω values at $\theta=0$ and $\theta=\pi/2$ obtained from (53) is more reasonable than the ratio of 30 to 1 calculated in either case from the spheroid assumption.

[22] P. A. Wolff, Phys. Rev. **95**, 56 (1954).

[23] C. Herring and M. H. Nichols, Revs. Modern Phys. **21**, 185 (1949); see also L. A. MacColl, Phys. Rev. **56**, 699 (1939), and Bell System Tech. J. **30**, 888 (1951).

We have assumed throughout that the final state density $N(\epsilon_k)$ is proportional to $\epsilon^{\frac{1}{2}}$. For the initial state density $N_c(\epsilon)$ more than one assumption has been made. In Fig. 8 are plotted three possible $N_c(\epsilon)$ functions for tungsten. The corresponding Auger transforms $T(\epsilon)$ are plotted in Fig. 9. Analytic expressions are given in Table III for $T(\epsilon)$ with $N_c(\epsilon)=k_1$ and $k_2\epsilon^{\frac{1}{2}}$. $T(\epsilon)$ for the Manning and Chodorow $N_c(\epsilon)$ function[24] was calculated on the analog computer. It differs so little from that for $N_c(\epsilon)=k_1$ that further calculation with it appeared unprofitable.

For pure Auger neutralization $N_i(\epsilon_k)$ functions have been determined in this way for $N_c(\epsilon)=k_1$ (Fig. 10 and $N_c(\epsilon)=k_2\epsilon^{\frac{1}{2}}$ (Fig. 11). $N_0(E_k)$ functions [$N_0=N_iP_e$ by (21)] have been obtained from these $N_i(\epsilon_k)$ functions using the probability of escape, P_e, of Eq. (52) corresponding to isotropic P_Ω. These are plotted in Figs. 12 and 13. The total electron yield, γ_N, which by (23) is the area under the $N_0(E_k)$ curve, has been calculated for each case and is given in Table IV where comparison is made with experimentally determined values for the slowest ions used.[7] The broadening effects and level shifts neglected here are least important at the lowest ion energies.

For pure Auger de-excitation $N_i'(E_k)$ functions for $N_c(\epsilon)=k_1$ have been determined and are shown in Fig. 14. $N_0'(E_k)$ functions obtained from these by use of the $P_e(\epsilon_k)$ function for isotropic P_Ω' [Eq. (52)] are plotted in Fig. 15. γ_D values (the areas under these curves) have been computed and are included in Table IV.

The energy extremes which the excited electrons may possess under the assumptions of this section may be seen in Figs. 10 through 15 or may be calculated directly from the energy relations (5) and (6) or (25) and (26) with $E(m-M)=E(m-M)=E(i-M)=0$. The metastable states involved here and throughout this paper are the lowest lying such states, $2s^3S$ for He, $ns[1\frac{1}{2}]^\circ$

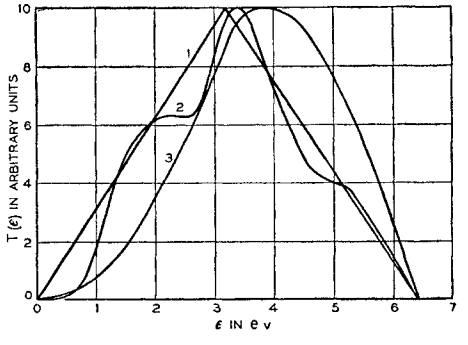

FIG. 9. Auger transforms obtained from Eq. (15) in the text from the $N_c(\epsilon)$ functions of Fig. 8. Curves 1, 2, and 3 here correspond to curves 1, 2, and 3 of Fig. 8, respectively. $T(\epsilon)$ is plotted in the figure to an arbitrary scale which makes $T(\epsilon)=10$ at its maximum in each case. Analytic expressions for curves 1 and 3 are to be found in Table III ($\epsilon_F=6.4$ ev). Curve 2 was obtained by numerical calculation on an analog computer.

[24] M. F. Manning and M. I. Chodorow, Phys. Rev. **56**, 787 (1939).

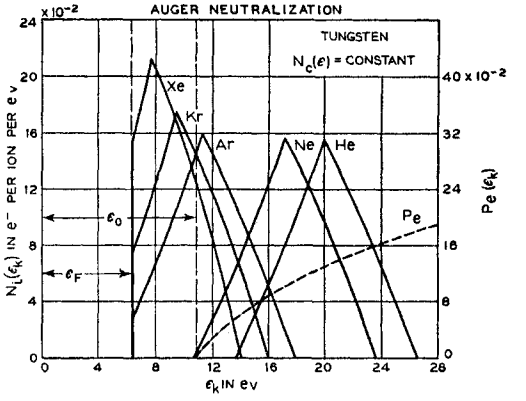

FIG. 10. Distributions in kinetic energy inside the metal, $N_i(\epsilon_k)$, of electrons excited by the Auger neutralization of the singly charged noble gas ions at a tungsten surface. $\epsilon_F=6.4$; $\varphi=4.5$; $\epsilon_0=10.9$ ev. Here $N_c(\epsilon)$ is assumed constant and no account is taken of atomic energy level shifts near the metal nor of the Heisenberg uncertainty principle. Areas under the $N_i(\epsilon_k)$ curves are normalized to one electron per incident ion. The escape probability function, $P_e(\epsilon_k)$, corresponding to isotropic distribution of electron velocities inside the metal [Eq. (52) in the text], is also plotted in this figure.

with $n=3$, 4, 5, and 6 for Ne, Ar, Kr, and Xe, respectively.

The above results exhibit a number of interesting features which we now discuss.

1. The forms of $N_0(E_k)$ and $N_0'(E_k)$ for Auger neutralization and de-excitation are seen to be quite different. The experimental energy distributions (Fig. 7 of reference 7, for example) certainly look more like the calculated curves for the neutralization process (Fig. 12) than those for the de-excitation process (Fig. 15) indicating the relative infrequency of resonance neutralization followed by Auger de-excitation. The details of form of the experimental distributions are not reproduced by the theory, it is true. The theoretical curves approach zero at the maximum energy much more abruptly than do the experimental curves.

2. The energy maxima in Figs. 12, 13, and 15 agree reasonably well with the experimental results for He^+, Ar^+, Kr^+, and Xe^+ (Fig. 7 of reference 7), but there appears to be no way to account for the anomalously high energy maximum observed experimentally for Ne^+ (Fig. 10 of reference 7).

3. The γ_N and γ_D values of Table IV show the experimentally observed decrease in passing through the sequence from He to Xe but the calculated values are all much too small. In the case of He the $N_i(\epsilon_k)$ distribution lies entirely at energies $\epsilon_k>\epsilon_0$. Variation of the form of $N_i(\epsilon_k)$ by variation of the $N_c(\epsilon)$ function (compare Figs. 10 and 11) cannot change γ_N much, as long as the area under the $N_i(\epsilon_k)$ curve is normalized to unity. The low theoretical γ_N for He is thus attributable only to the $P_e(\epsilon_k)$ function used. For Ar, Kr, and Xe where the $N_i(\epsilon_k)$ distribution lies partly above and partly below $\epsilon_k=\epsilon_0$, the form of $N_i(\epsilon_k)$ as determined by

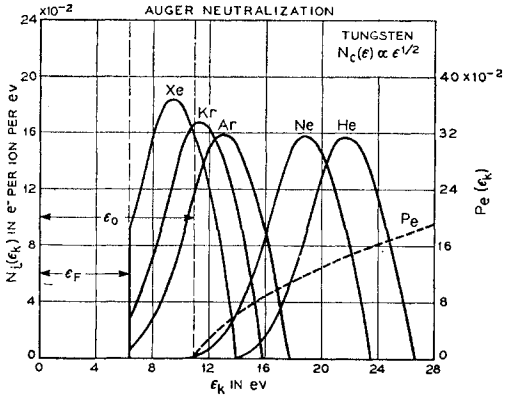

FIG. 11. $N_i(\epsilon_k)$ functions for $N_c(\epsilon) \propto \epsilon^{\frac{1}{2}}$, other conditions and assumptions the same as those for Fig. 10. The same $P_e(\epsilon_k)$ function is plotted here as in Fig. 10.

$N_c(\epsilon)$ has greater effect on γ_N as is to be seen in Table IV.

4. Table IV indicates that γ_D is larger than γ_N. Thus we expect the two-stage process of resonance neutralization followed by Auger de-excitation to be more productive of secondary electrons per incident ion than direct Auger neutralization of the incident ion.

5. The $N_0(E_k)$ functions and γ values derived above are independent of kinetic energy of the incident particle since this energy enters in no way into the theory. Although this state of affairs is in general agreement with the experiment we are as yet unable to account for the finer details of the observed energy dependence.

VIII. ATOMIC ENERGY LEVEL SHIFTS NEAR THE METAL

The variation of atomic energy levels near the metal surface is accounted for in the theory of Secs. III and IV by inclusion of the interaction energy terms, $E(n-M)$, $E(i-M)$, and $E(m-M)$. These terms appear in the effective ionization energy [Eq. (6)] and effective excitation energy [Eq. (26)]. In the treatment of Sec. VII these terms were neglected. We wish now to discuss these terms and to estimate their values for inclusion in the theory.

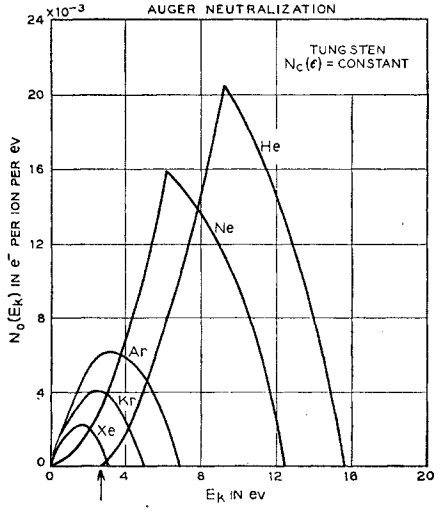

FIG. 12. $N_0(E_k)$ functions derived from the $N_i(\epsilon_k)$ and $P_e(\epsilon_k)$ functions of Fig. 10. The minimum energy in the He distribution is indicated by the arrow on the E_k axis. γ_N values (areas) derived from these curves are given in Table IV.

Since the interaction between an atomic particle and a metal surface certainly cannot be said to be well known it is perhaps to the point to begin this discussion by pointing out that the basic results which follow from inclusion of the interaction terms are insensitive to the specific estimates of their values. There are two basic experimental results which we wish to explain by including the interactions with the metal as well as the effects of the Heisenberg uncertainty principle. These are: 1. the observed departures in form of the observed $N_0(E_k)$ functions from those determined in the preceding section, in particular the observation of appreciable numbers of electrons beyond the energy limit $E_x - \varphi \simeq E_i - 2\varphi$ for Ne^+ on tungsten, and 2. the relative infrequency of the two-stage process of resonance neutralization followed by Auger de-excitation. It will be seen that these results can be explained if we may assume: 1. that the image force attraction between the ion and the metal is operative, and 2. that the repulsive forces for the particles ion, normal atom, and metastable atom become appreciable at distances from the metal which are in the same sequence as the diameters of the particles. It is submitted that each of these demands is reasonable. Beyond this it is the author's opinion that reasonable estimates for the important interaction terms can in fact be made. These enable one to derive approximate quantitative results from the theory.

TABLE IV. γ_N and γ_D values obtained from the calculated energy distributions assuming no atomic energy level shifts, isotropic P_Ω, and neglecting the Heisenberg principle (Figs. 12, 13, and 15).

Atom	γ_N $N_c(\epsilon)$ = const (Fig. 12)	γ_N $N_c(\epsilon) \propto \epsilon^{\frac{1}{2}}$ (Fig. 13)	γ_D $N_c(\epsilon)$ = const (Fig. 15)	Measured γ_i for 10-ev ions
He	0.136	0.142	0.155	0.293
Ne	0.103	0.114	0.129	0.213
Ar	0.028	0.040	0.063	0.094
Kr	0.013	0.021	0.038	0.047
Xe	0.0044	0.0065	0.017	0.018

The interaction of an atomic particle with a metal surface may be thought to be compounded of the following possible components:

1. the Coulombic image force attraction for ions,
2. the van der Waals attraction resulting from the particle's polarizability,
3. a possible exchange force of the type responsible for the covalent bond, and

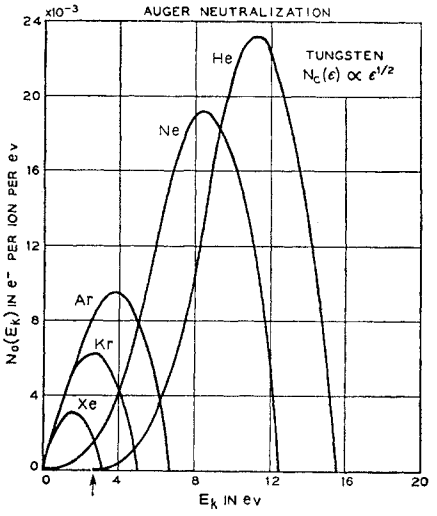

FIG. 13. $N_0(E_k)$ functions derived from the $N_i(\epsilon_k)$ and $P_e(\epsilon_k)$ functions of Fig. 11. The minimum energy in the He distribution is indicated by the arrow on the E_k axis. γ_N values derived from these curves are given in Table IV.

4. the repulsion resulting from interpenetration of the electron clouds and the Pauli principle.

We proceed to discuss these forces in turn.

The *image potential* is

$$-e^2/4s = -3.6/s \text{ ev}, \tag{56}$$

where s is in A.[25]

For the *van der Waals interaction* between an atomic particle and a metal we use the expression derived by Prosen and Sachs,[26]

$$-(2\pi)^{-3}\alpha e^2 \pi k_m^2 s^{-2} \ln(2k_m s). \tag{57}$$

TABLE V. Polarizabilities for normal atoms (α_n) and metastable atoms (α_m) of the noble gases.

	$10^{25}\,\alpha_n$ (cm³)[a]	$10^{25}\,\alpha_m$ (cm³)[b]
He	2.16	57
Ne	3.98	76
Ar	16.3	230
Kr	24.3	280
Xe	40.1	410

[a] Determined from measurements of the dielectric constant. Landolt-Börnstein, *Tables* (Julius Springer, Berlin, 1950), sixth edition, Vol. I, Part I, p. 401.

[b] These estimates are obtained as $\alpha_n[E_i/(E_i-E_x)]^2$, which expression is derived from Margenau's formula (reference 27) for the static polarizability by assuming equal oscillator strengths, $\Delta = E_i$ for the normal atom, and $\Delta = E_i - E_x$ for the metastable atom. It is interesting to note that the assumption that α is proportional to volume gives α_m values of 40, 59, 261, 332, 436 for He^m, Ne^m, Ar^m, Kr^m, and Xe^m, respectively, by using the diameters given in Table VI.

[25] R. G. Sachs and D. L. Dexter, J. Appl. Phys. **21**, 1304 (1950), have discussed the quantum limits on the electrostatic image force and conclude that this classical expression is accurate if the distance from the surface is larger than the lattice constant. Although the classical expression is used here, the magnitude of the image potential very close to the surface is not involved in any conclusions of the theory.

[26] E. J. R. Prosen and R. G. Sachs, Phys. Rev. **61**, 65 (1942).

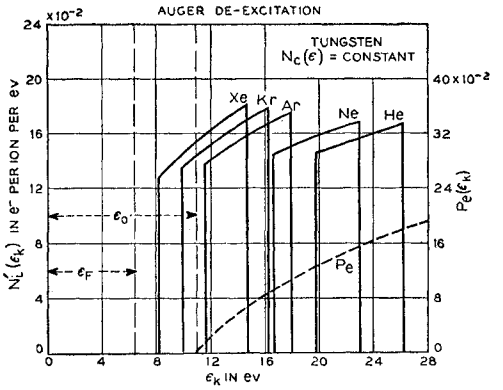

FIG. 14. Distributions in kinetic energy, $N_i'(\epsilon_k)$, of electrons excited by the Auger de-excitation at a tungsten surface of the least energetic metastable atoms of the noble gases. $N_c(\epsilon)$ is taken as constant and the effects of atomic energy level shifts near the metal and the Heisenberg uncertainty principle are neglected. The $N_i'(\epsilon_k)$ functions are normalized to an area of one electron per incident metastable atom. The probability of escape function, P_e, plotted here is the same as that used for Auger neutralization in Figs. 10 and 11.

Here α and k_m are the polarizability of the atom and the wave number of the fastest electron in the metal, respectively.

For free electrons $k_{\max} = (2m\epsilon_F)^{\frac{1}{2}}/\hbar$. Using Manning and Chodorow's value[24] for $\epsilon_F = 0.47$ ry $= 6.4$ ev, we calculate $k_m = 1.3\times10^8$ cm^{-1}. Manning and Chodorow plot curves of ϵ *vs* k from which it appears that at $\epsilon = 0.47$ ry, $\theta \sim 45°$ or $k_m \sim 1\times10^8$ cm^{-1}. This latter value is used in expression (57), which on evaluation of other constants becomes

$$-1.83\times10^{23}\alpha s^{-2}\ln(2s) \text{ ev}, \tag{58}$$

with s in A and α in cm³. Values for the polarizabilities used in this expression are given in Table V. The

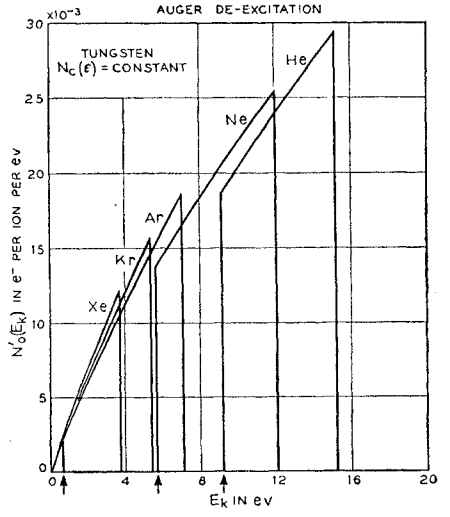

FIG. 15. $N_0'(E_k)$ functions derived from the $N_i'(\epsilon_k)$ and $P_e(\epsilon_k)$ functions of Fig. 14. The minimum energies in the distributions for He^m, Ne^m, and Ar^m are indicated on the E_k axis. γ_D values derived from these curves are given in Table IV.

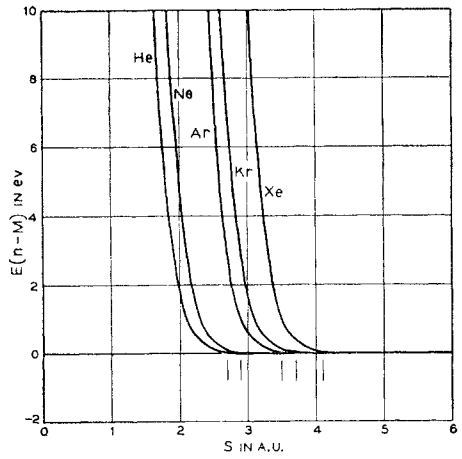

FIG. 16. Plots of the energy of interaction of normal noble gas atoms with a tungsten surface estimated by the methods described in the text [Eq. (60)].

polarizability of the ion is so small that its van der Waals force is neglected in this work. A means of estimating polarizabilities for the metastable atoms based on a formula of Margenau[27] is indicated in footnote b to Table V.

The exchange force listed as the third possible interaction component need be considered only for the metastable atom and the ion. The fact is that we know nothing about it for these cases. We shall proceed as though it does not exist on the grounds that even if it does the interaction need not occur in a bonding state on every encounter. One may point to the analogy of the possible bonding and antibonding states on approach of two atoms to form a diatomic molecule. If some

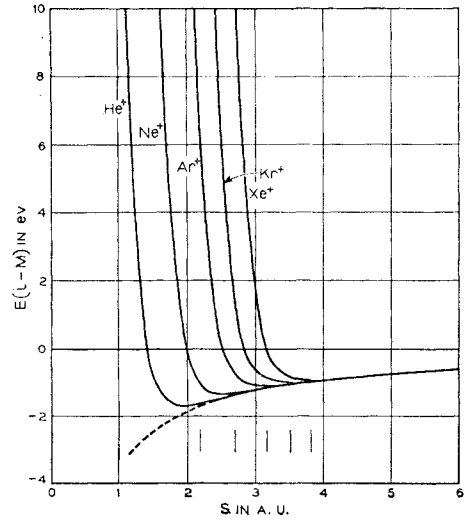

FIG. 17. Plots of the energy of interaction of noble gas ions with a tungsten surface estimated by the procedures discussed in the text [Eq. (61)]. The dashed line indicates the extension of the image potential term only.

[27] H. Margenau, Revs. Modern Phys. **11**, 1 (1939), formula (C9).

encounters result in the "bonding" state our estimates from the experimental data of the partition between Auger neutralization and de-excitation (Sec. XIV) will be in error in the direction of underestimating the fraction of de-excitations.

For ions and normal atoms we represent the repulsive energy by the one-dimensional exponential $B\exp(-bs)$. This appears justified in view of the fact that such a form adequately represents the repulsive interaction of atoms in crystals, e.g., the alkali halides,[28] as well as free atoms.[29,30] We assume a value of 5×10^8 cm$^{-1}=5$ A^{-1} for b for all ions (b_i) and normal atoms (b_n). (Table VII, footnote a.) We expect a lower value of b for the metastable atom (b_m) because it has a smaller electron density in its outer portions. A value of 1.5 A^{-1} has been estimated (Table VII, footnote b). Furthermore, it is evident that a single exponential cannot represent adequately the repulsive interaction for the metastable atom. On sufficiently close approach the interaction of

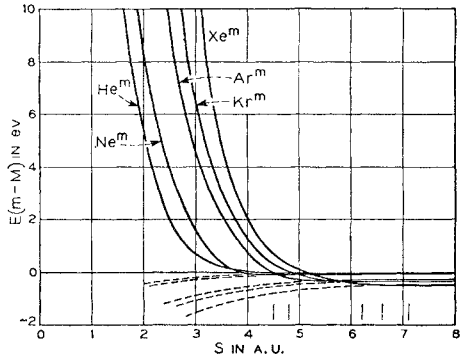

FIG. 18. Plots of the energy of interaction of metastable atoms with a tungsten surface estimated by the methods given in the text [Eq. (62)]. The dashed lines indicate the extensions of the van der Waals terms only.

ion, normal atom, and metastable atom should all approach the same interaction, namely that of the atomic core. Thus a low value of b_m can characterize the metastable interaction only at larger values of s. For these reasons the metastable repulsion is compounded of two exponentials as indicated below.

For given b the value of B in the term $B\exp(-bs)$ determines the distance from the metal at which the repulsive interaction becomes large. Absolute values cannot be determined with accuracy, but one should be able to estimate relative values which are reasonably good. Any method adopted for estimating B may be taken to define a distance scale. The procedure used here is the following. A distance s_0 at which the atomic particle "touches" the metal surface is defined as

$$s_0=d/2+a_i/2, \tag{59}$$

[28] M. Born and J. E. Mayer, Z. Physik **75**, 1 (1932).
[29] J. C. Slater, Phys. Rev. **32**, 339 (1928).
[30] W. E. Bleick and J. E. Mayer, J. Chem. Phys. **2**, 252 (1934).

the sum of the particle's radius and half the lattice constant of the metal. One makes the energy of repulsive interaction at this distance equal to that calculated by Bleick and Mayer[30] for the interaction of two free Ne atoms when separated by the viscosity diameter (Table VI) of the Ne atom. The procedure is admittedly arbitrary but should define a reasonable relative distance scale.

The theoretical Ne−Ne interaction [$1.18\times10^4\times\exp(-4.8r)$ ev, r in A] amounts to 0.044 ev at $r=2.59$ A. Here we have assumed the repulsive interaction to be 0.05 ev at $s=s_0$. With the values of b and d estimated above, the B values listed in Table VII have been obtained.

For the value of a_l to be used in Eq. (59), the edge length of the fundamental cube in the metal lattice, we have takent he value of 3.16 A for tungsten.[31] The values of s_0 obtained from Eq. (59) with the diameters of Table VI are indicated in Figs. 16, 17, and 18 by the short vertical lines. In each case they are to be identified from left to right with He, Ne, Ar, Kr, and Xe, in that order.

The interactions with the metal used in the present work may now be summarized. For the normal atom the van der Waals attraction turns out to be negligible [0.014 ev for He at 2 A, 0.095 ev for Xe at 4 A]. Thus we take

$$E(n-M)=B_n\exp(-b_ns), \tag{60}$$

with B_n and b_n given in Table VII. These interaction energies for He, Ne, Ar, Kr, and Xe are plotted in Fig. 16.

For the ion, $E(i-M)$ comprises the image force and repulsive interactions. Thus,

$$E(i-M)=B_i\exp(-b_is)-3.6/s. \tag{61}$$

These interaction energies are plotted in Fig. 17.

The metastable atom-metal interaction, $E(m-M)$, comprises three terms: (1) the repulsive term operating at larger distances, (2) the repulsive term representing the effect of the atomic core as discussed above, and (3) the van der Waals interaction which is appreciable. Thus, from Eq. (58), using the polarizability of the metastable atom we obtain

$$E(m-M)=B_m\exp(-b_ms)+B_i\exp(-b_is)-1.83\times10^{23}\alpha_ms^{-2}\ln(2s). \tag{62}$$

These interactions are plotted in Fig. 18.

The interaction energies of Eqs. (60), (61), and (62) have been used in determining the effects of energy level shifts on the resonance and Auger transitions which occur when an atomic particle is near a metal surface. The fact that a better understanding of the phenomena results lends credibility to the interaction energies derived here.

[31] R. W. G. Wyckoff, *Crystal Structures* (Interscience Publishers, Inc., New York, 1951), Table II, 4.

TABLE VI. Particle diameters for normal atoms (d_n), metastable atoms (d_m), and ions (d_i) of the noble gases.

	$d_n(A)$	$d_m(A)$	$d_i(A)$
He	2.19[a]	5.8[b]	1.3[e]
Ne	2.57[a]	6.4[c]	2.3[f]
Ar	3.66[a]	9.2[c]	3.3[f]
Kr	4.18[a]	10.0[d]	3.8[f]
Xe	4.93[a]	10.9[c]	4.4[f]

[a] Viscosity diameter from Landolt-Börnstein, *Tables* (Julius Springer, Berlin, 1950), sixth edition, Vol. 1, Part I, p. 325.
[b] Estimated from the extension of the calculated electron density functions for unexcited H(1s) and excited H(2s). From Fig. 20 of G. Herzberg, *Atomic Spectra and Atomic Structure* (Dover Publications, New York, 1944), second edition, we conclude $d_n[H(2s)]\simeq2.6d_n[H(1s)]$. Since $r\propto1/Z$, $d_n[H(2s)]\simeq5.2d_i[He^+]$. If we take account of the incomplete shielding of the nucleus in the case of He^m by assuming $d\propto(E_i)^{-\frac{1}{4}}$, then $d_m[He^m]=(3.4/4.77)^{\frac{1}{4}}d_n[H(2s)]$ and $d_m[He^m]\simeq4.5d_i[He^+]$.
[c] From the ratio of d_m/d_n given by J. P. Molnar, Phys. Rev. **83**, 940 (1951) using the viscosity d_n.
[d] Interpolated between the values for Ar and Xe.
[e] Obtained from the viscosity diameter of H (reference a) taking $r\propto1/Z$. Thus $d[He^+]=d[H]/2=1.26$ A.
[f] Taken as $0.9d_n$.

IX. EFFECT OF LEVEL SHIFTS ON THE AUGER TRANSITIONS

Having in our possession what are at least plausible potential curves representing the interactions of noble gas atoms and ions with a metal surface, we may proceed to discuss the Auger transitions in terms analogous to those used in the discussion of electronic transitions in diatomic molecules. The procedure is to place the potential curves properly on an energy-distance plot and to discuss the Auger transitions as jumps between these curves which obey the Franck-Condon principle.

Consider first the process of Auger neutralization. In Eq. (4) the process was written for the system of the incoming ion and two interacting electrons in the metal transforming itself to the isoelectronic system of the normal atom and a free electron. We find it more convenient here to consider the system comprising the incoming ion and all electrons in the metal (taken as n in number) which is transformed to the isoelectronic system of the neutralized atom, a free electron, and $(n-2)$ electrons remaining in the metal. Thus we write

TABLE VII. Values of parameters B and b in the repulsive interaction term: $B\exp(-bs)$.

	$b_n=5A^{-1}$,[a] $b_m=1.5A^{-1}$,[b] $b_i=5A^{-1}$,[a]		
	$10^{-5}B_n$ (ev)	$10^{-2}B_m$ (ev)	$10^{-5}B_i$ (ev)
He	0.36	0.43	0.03
Ne	0.99	0.67	0.36
Ar	19.8	5.5	4.45
Kr	54.8	10.0	19.8
Xe	398.0	20.0	88.5

[a] Theoretical attempts to explain the data of J. K. Roberts, Proc. Roy. Soc. (London) **A129**, 146 (1930); **A135**, 192 (1932), on the temperature variation of the accomodation coefficient for interaction of an atom and a metal have yielded $b=4A^{-1}$ [J. M. Jackson and A. Howard, Proc. Roy. Soc. (London) **A142**, 447 (1933)] and $2A^{-1}$ [A. F. Devonshire, Proc. Roy. Soc. (London) **A158**, 269 (1937)]. The interaction in solids (alkali halides) gives $b=2.9A^{-1}$ (reference 28), between free He atoms, $4.6A^{-1}$ (reference 29), and free Ne atoms, $4.8A^{-1}$ (reference 30).
[b] Estimated on the basis that equal repulsive forces arise when there is equal overlap of charge between the metal and the atomic particle.

the Auger neutralization process as

$$X^+ + ne_M^- \rightarrow X + e^- + (n-2)e_M^-. \qquad (63)$$

The energy of the system $X^+ + ne_M^-$ with X^+ at rest at $s=\infty$ is a discrete value, taken to be zero. The system $X + e^- + (n-2)e_M^-$ with $X + e^-$ at rest at $s=\infty$ may assume a band of energies corresponding to the n^2 possible choices of energy levels in the metal from which the two electrons are drawn. This band extends from $-(E_i - 2\epsilon_0)$ to $-(E_i - 2\varphi)$ below the zero level as just defined. These energy limits may be derived by considering the energy transformations in carrying out the process of Eq. (63) at $s=\infty$. As s decreases toward zero the energy of the system $X^+ + ne_M^-$ varies as $E(i-M)$ [see Fig. 17], that of $X + e^- + (n-2)e_M^-$ as $E(n-M) - (E_i - \alpha - \beta)$ [see Fig. 16]. The potential curves relevant to the Auger neutralization of He^+ on tungsten are shown in Fig. 19.

The curves of Fig. 19 are potential energy curves which are independent of the kinetic energy of the particles in the system. The total energy of the system including kinetic energy would be represented by a horizontal line at $E_t = E_{k\infty}(He^+)$ on the ordinate scale of Fig. 19. At any value of s, $E_k(He^+)$ is the energy distance from this total energy line to curve 1. The energy interval between a point on a curve in the band between curves 2 and 3 and the total energy line is $E_k(He) + E_k(e^-)$. We assume that the Franck-Condon principle holds. Thus transitions occur vertically at constant $s = s_t$ on a plot such as Fig. 19, and $E_k(He^+)$ immediately before the transition equals $E_k(He)$ just after the transition. Thus $E_k(e^-)$, the kinetic energy which the escaping electron assumes outside the metal, is the energy interval at the distance s_t between curve 1 and some curve lying between 2 and 3 in Fig. 19. This

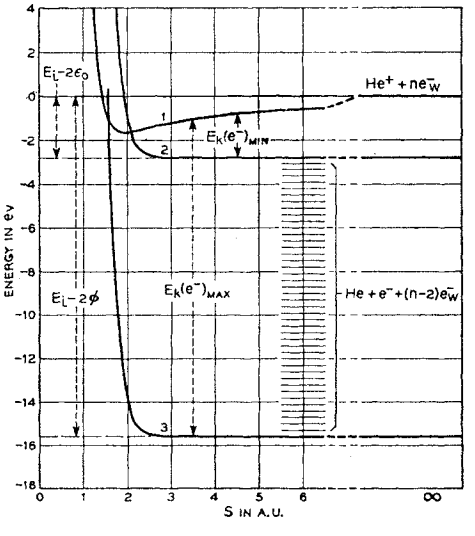

FIG. 19. Potential curve diagram appropriate to the Auger neutralization of He^+ at a tungsten surface. The process is that given in Eq. (63) in the text.

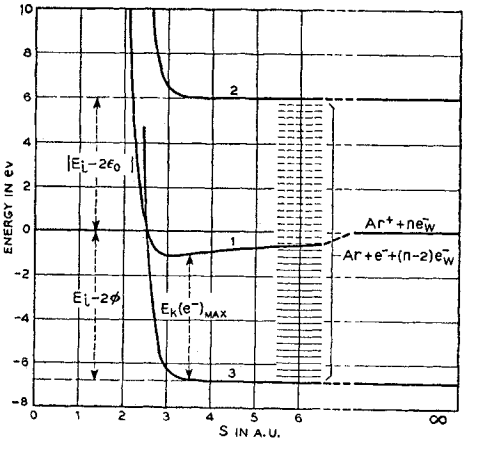

FIG. 20. Potential curve diagram appropriate to the Auger neutralization of Ar^+ at a tungsten surface.

conclusion leads, of course, to the same energy condition as relation (5) when E_k is transformed to ϵ_k by Eq. (3).

The potential curve diagram appropriate to Auger neutralization of Ar^+ is shown in Fig. 20. This is an example of the situation which prevails when $E_i - 2\epsilon_0 < 0$. Curve 1 lies imbedded in the continuum of levels between curves 2 and 3. Only those final states which lie below curve 1 are available for the transition. $E_k(e^-)$ is seen to have a minimum value of zero at all s.

Potential curve diagrams for Auger de-excitation of a metastable atom may be drawn and interpreted in a similar fashion; that appropriate to the de-excitation of Ne^m is shown in Fig. 21. Here the process is written in the form,

$$X^m + ne_M^- \rightarrow X + e^- + (n-1)e_M^-. \qquad (64)$$

The energy conditions (25) and (26) fix the relative positions of the potential curves in this case and the kinetic energy of the ejected electron is again the vertical distance from curve 1 to a curve in the band between curves 2 and 3, at the distance at which the transition occurs.

It is now clear what the effect of inclusion of energy level shifts near the metal has upon the Auger processes, in particular on the energy limits of ejected electrons. From Figs. 19 and 20 it is evident that for a given Auger neutralization process both $(E_k)_{min}$ and $(E_k)_{max}$ decrease as the distance s_t at which the process occurs decreases and are at no distance larger than the limits at $s=\infty$. This amounts to shifting the $N_i(\epsilon_k)$ functions like those of Figs. 10 and 11 lower on the ϵ_k scale. In the case of Auger de-excitation, on the other hand, Fig. 21 indicates that the energy extrema increase if the transition takes place close to the metal. This results from the fact that the potential curve for the metastable atom rises above its asymptote at larger values of s than does that for the normal atom. If one takes no account of effects which broaden the energy

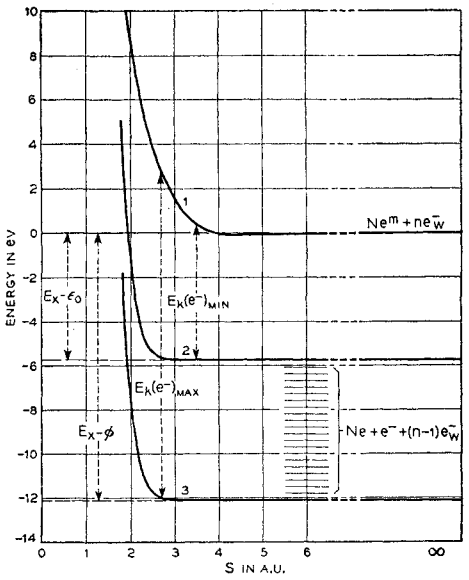

FIG. 21. Potential curve diagram appropriate to the Auger de-excitation of He^m at a tungsten surface. The process is that of Eq. (64) in the text.

distributions one determines from the potential curve diagrams the kinetic energy maxima shown in Fig. 22 for Auger neutralization of Ne^+ (curve 1) and Auger de-excitation of Ne^m (curve 2). It is evident that a means of accounting for the observed violation of the energy limit $E_i-2\varphi \simeq E_x-\varphi$ in the case of Ne^+ is provided by the process of Auger de-excitation.

The energy level shifts depicted by the potential curves of Figs. 19, 20, and 21 are incorporated into the theory of Secs. III and IV in the effective ionization and excitation energies defined in Eqs. (6) and (26). These energies may be evaluated from the interaction energies of Eqs. (60), (61), and (62) or from Figs. 16, 17, and 18. This has been done for the effective ionization energy. The results, plotted as (E_i-E_i') *vs* s are shown in Fig. 23. From the equations referred to we derive

$$(E_i-E_i')=E(n-M)-E(i-M)$$
$$=B_n\exp(-b_ns)-B_i\exp(-b_is)+3.6/s. \quad (65)$$

E_x' functions have not been plotted. E_x' has been used, however, to fix the effective metastable energy level as is discussed in the next section.

X. EFFECT OF LEVEL SHIFTS ON THE RESONANCE TRANSITIONS

We discuss in this section the effect of energy level shifts on the resonance neutralization of ions and the resonance ionization of atoms near a metal surface. For noble gases these processes must involve excited atoms. In what follows the excited level is designated by the metastable atom notation even though resonance processes near a metal surface are not restricted to metastable states. Resonance neutralization is written as

$$X^++e_M^-(-\alpha)\rightarrow X^m, \quad \varphi<\alpha<\epsilon_0, \quad (66)$$

resonance ionization as

$$X^m\rightarrow X^++e_M^-(-\alpha), \quad \alpha<\varphi. \quad (67)$$

Here we consider the system of the ion and one electron in the metal and the isoelectronic system of the neutralized metastable atom.

If we balance energies on the two sides of either of these equations we obtain for α,

$$\alpha=E_i'-E_x'$$
$$=E_i-E_x+E(i-M)-E(m-M). \quad (68)$$

Equation (68) expresses the resonance nature of the transition.

If energy level shifts near the surface are neglected (68) reduces to $\alpha=E_i-E_x$ and one expects resonance neutralization to be possible only if $\varphi<E_i-E_x<\epsilon_0$. Resonance ionization of the metastable atom, X^m, is then possible only if $E_i-E_x<\varphi$. Under this assumption we expect only He^+ and Ne^+ of the singly charged ions of the noble gases to be neutralized at a tungsten surface by the process (66) and only Ar^m, Kr^m, and Xe^m to be ionized at a tungsten surface by the process (67) (see Table II).

If we include the interaction terms $E(i-M)$ and $E(m-M)$ and assume that the Franck-Condon principle holds, α becomes a function of s. Thus, from expressions (61) and (62) in (68),

$$\alpha=E_i-E_x-3.6/s+1.83\times10^{23}\alpha_m s^{-2}\ln(2s)$$
$$-B_m\exp(-b_ms). \quad (69)$$

The Franck-Condon principle is implied in writing Eq. (69) since we evaluate $E(i-M)$ and $E(m-M)$ at the same value of s and neglect translational energy of the atom. This amounts to assuming that the electronic transition affects neither position nor momentum of the atomic particle.

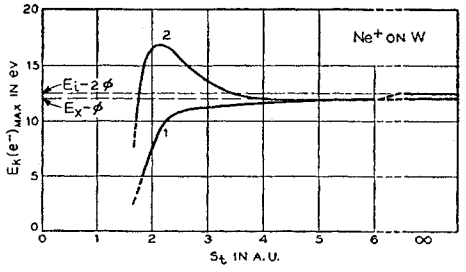

FIG. 22. Kinetic energy maxima as a function of distance s_t at which the transition occurs for Auger neutralization of Ne^+ (curve 1) and Auger de-excitation of Ne^m (curve 2) at a tungsten surface, no account being taken of effects which broaden the distributions. Note the fact that Auger de-excitation can yield electrons whose external energies may exceed the limit $E_x-\varphi$ calculated on the basis of no atomic energy level shifts.

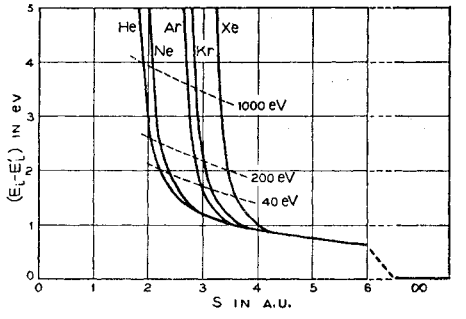

FIG. 23. Plot of (E_i-E_i'), the change in effective ionization energy near the metal surface, as a function of distance from the surface. The lower part of each curve which is common to all curves represents the effect of the image potential of the ion outside the metal. The dashed lines are the loci of $E_i-E_i'(s_m)$ for ions of the incident kinetic energies indicated.

As s decreases from large values toward zero α decreases, since the image potential term, $-3.6/s$, at larger s and the exponential term at closer approach predominate over the van der Waals term. The distance at which $\alpha=\varphi$ is a critical distance, s_c, since resonance neutralization is possible only for $\alpha>\varphi$, $s>s_c$, whereas resonance ionization is possible only if $\alpha<\varphi$, or $s<s_c$.[32] We neglect the small population of states in the metal above the Fermi level at temperatures above absolute zero.

It is possible to plot potential curve diagrams descriptive of the resonance processes which are the analogs of those plotted in Figs. 19, 20, and 21 for the Auger processes.[6,32] A more convenient plot perhaps is that of Fig. 24 in which $-(E_i'-E_x')=-\alpha$ [from Eqs. (68) and (69)] is plotted as a function of s. The energy band structure in tungsten in indicated to the left of the $s=0$ axis in Fig. 24. The critical distances (s_c) for He^m and Ne^m are indicated by the arrows labeled 1 and 2, respectively.

It is clear that the variation of energy levels near a metal surface further restricts the possibility of resonance neutralization of noble gas ions. The process is possible only if the probability distribution function for the process, $P_t''(s,v_0)$, has become appreciable in the region $s>s_c$. In Fig. 24 a $P_t''(s,v_0)$ function is placed at what appears a reasonable value of $s_m(\sim 5A)$ for ions of about 40 ev energy.[33] Since s_c for He appears to be some 12 A or more it is evident that He^+ cannot be neutralized by resonance capture at a tungsten surface. Resonance neutralization appears possible, however, for Ne^+. Thus for electron ejection from clean tungsten by singly charged noble gas ions one need consider the role of resonance transitions only in the case of Ne^+. This can be shown to be in accord with the experimental facts.

[32] The basic ideas concerning the critical distance, s_c, and some of its implications have already been published (reference 6). L. J. Varnerin, Jr., Phys. Rev. **91**, 859 (1953), has recognized independently that inclusion of the image potential yields the critical distance, s_c.

[33] D. Sternberg (private communication).

XI. MULTISTAGE EJECTION PROCESSES FOR INCIDENT IONS AND METASTABLE ATOMS

Calculations by Shekhter[3] and by Cobas and Lamb[4] (see Table X) indicate that at a given distance from the surface the transition rate for the resonance processes is considerably larger than those for the Auger processes. If this is the case, an atomic particle approaching a metal is first subject to a resonance transition, if such is possible, and later, on closer approach, to an Auger transition. This state of affairs is necessary if so-called multistage ejection processes are to be possible. It appears that we must postulate these if some of the experimental data are to be explained.

In a possible two-stage process of electron ejection by an incoming ion the ion is first neutralized to an excited level by resonance capture and the excited atom so formed subsequently decays to the ground state with excitation of an internal secondary electron in a process of Auger de-excitation. It is clear that the further restrictions which variation of energy levels near the metal impose upon the resonance process make the two-stage ejection process less likely. The interpretation of the experimental results for noble gas ions on clean tungsten bear this out.

A two-stage electron ejection process for incident metastable atoms is also possible. In it the metastable atom is first resonance ionized and the ion so formed subsequently neutralized in an Auger process. The conditions which make resonance neutralization less probable make resonance ionization more probable and it is evident that metastable atoms of the noble gases incident on metals will, for the most part, eject electrons by the two-stage process. Thus ejection by incident ions or metastable atoms should be essentially indistinguishable. This conclusion is in accord with the experimental facts but seems not to have been recognized by previous investigators using incident metastable atoms. Thus the energy distributions measured by Greene[34] for incident metastable atoms look much like those characteristic of Auger neutralization (Figs. 12, 13, and 28) and not like those characteristic of Auger de-excitation (Fig. 15). The observation of a minimum electron energy at or near zero which Greene had difficulty in explaining in terms of Auger de-excitation then becomes reasonable. For a clean surface of tungsten it is evident (see below) that even for neon most slow incident metastable atoms will be resonance ionized before the Auger processes become very probable.

When atomic energy level shifts with s are taken into account and when the critical distance s_c, defined in Sec. X, lies in the range in which the resonance processes are possible there arises the interesting possibility of a three-stage ejection process for incident ions in which an incoming ion is first resonance neutralized at $s>s_c$ then resonance ionized at $s<s_c$, and finally Auger

[34] D. Greene, Proc. Phys. Soc. (London) **B63**, 876 (1950).

neutralized. The fraction of the incoming ions which finally participate in Auger neutralization and the complementary fraction involved finally in Auger de-excitation will now depend quite critically on the specific value of s_c, the transition rate functions for the resonance and Auger processes, as well as the incident velocity, v_0, of the atomic particle. The solution of the problem is somewhat involved but can be done with only minor restrictive assumptions. One can obtain an adequate picture of what happens from the simplified version which is included here.

We shall assume that the Auger processes of neutralization and de-excitation occur instantly when the particle reaches a given distance, s_A, assumed to be the same for the two processes. The fraction of Auger neutralization processes is then the probability $P_0(s_A,v_0)$ that an incoming ion reach s_A as an ion. $1-P_0(s_A,v_0)$ then gives the fraction of Auger de-excitations. The P_0 function follows directly from a consideration of the resonance processes. For $s>s_c$ ions may turn to metastable atoms by resonance neutralization and the population of ions in the incoming beam decays according to the P_0 function of Eq. (43) with parameters characterizing the resonance processes. For $s<s_c$ resonance neutralization is no longer possible but metastable atoms formed from ions in the region $s>s_c$ may now turn back to ions by resonance ionization. The population of ions then increases again with decreasing distance. The probability, P_0, that the incident particle is an ion at the distance s can be shown to be

$$\begin{aligned} P_0(s,v_0) &= \exp\{-\exp[-a''(s-s_m'')]\}, \quad s>s_c, \\ &= 1+\{1-\exp[-a''(s_c-s_m'')]\} \\ &\quad \times\exp\{-\exp[-a''(s-s_m'')]\}, \quad s<s_c. \end{aligned} \tag{70}$$

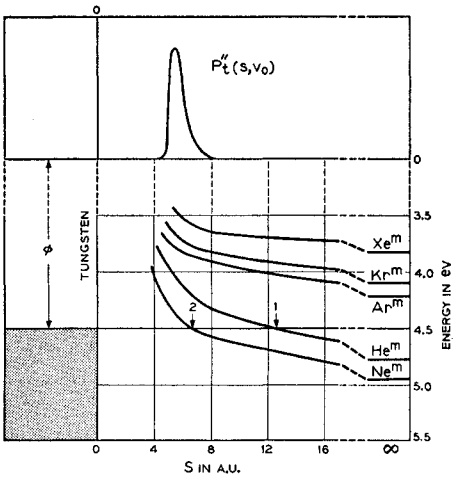

FIG. 24. Plot of the variation of the metastable levels (lowest lying) of He, Ne, Ar, Kr, and Xe with distance outside a tungsten surface. The filled portion of the conduction band in tungsten is indicated by stippling. The critical distances (s_c) for He^m and Ne^m are indicated at 1 and 2, respectively. A representative $P_t''(s,v_0)$ function for resonance ionization is shown at the top of the figure.

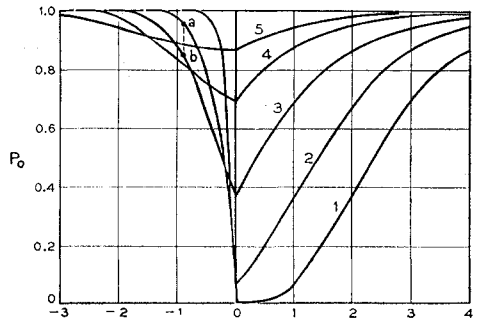

FIG. 25. Plots of the probability, $P_0(s,v_0)$, that an incident ion remains an ion for the case in which the critical distance s_c lies in the range of s where the resonance processes are probable. The Auger processes are neglected in these plots. Curves 1 through 5 are for increasing incident velocity v_0 in that order, the velocity ratio between adjacent curves being e. For curve 3 the incident velocity is such that $s_m=s_c$.

The P_0 function from (70) is plotted in Fig. 25 for various incident velocities. Two conclusions may be drawn from the figure: 1. Inasmuch as the rise in P_0 at $s<s_c$ is rapid we expect a relatively low percentage of incident particles to remain metastable atoms long enough to become de-excited by Auger de-excitation. This result is in accord with the experiment which indicates that a high percentage of incident Ne^+ ions do finally reach the atomic ground state via the Auger neutralization process (Sec. XIV). 2. Increase in velocity of the incoming particle should *increase* the fraction of incident ions which participate in the two-stage ejection process. Thus if the Auger processes occur at a distance $s_A<s_c$ such that, as an example, $a''(s_A-s_c)=-0.9$ in Fig. 25, an increase in velocity of a factor of e from curve 2 to curve 3 will decrease the fraction of ions at s_A from 0.95 (point a) to 0.85 (point b). This is the result of the interesting cross-over of the curves of Fig. 25 at $s<s_c$. This is a manifestation of the fact that slower particles are transformed in larger proportion from ions to metastable atoms for $s>s_c$ but revert more rapidly to ions at $s<s_c$ than do faster particles. This effect makes it possible to account for the observed variation of γ_i for Ne^+ on tungsten as is explained in Sec. XV. A calculation of the P_0 function based on the inclusion of an exponential rate function for the Auger processes as well as the resonance process has been shown to preserve this variation with velocity for suitably chosen parameters defining the two rate functions and the critical distance, s_c.

The variation of energy levels does not make possible a three-stage ejection process for incident metastable atoms because resonance ionization can succeed but not precede resonance neutralization as distance between atom and metal decreases. Thus incident metastable atoms remain such till the distance s_c is reached after which they may turn to ions. If s_c lies in the range of s in which the resonance processes occur but the Auger processes have not yet become probable, this transformation, as Fig. 25 indicates, is so rapid that a large

proportion of the incident metastables do become ions before the Auger processes set in. Thus, as indicated above, Auger de-excitation of a metastable atom of a noble gas at a metal surface is a rare occurrence under any circumstances.

In the above discussion it has been assumed that when Auger neutralization and Auger de-excitation are both possible they may be treated as individual competing processes. In quantum-mechanical terms this means that we are assuming the wave functions of the participating electrons to be either purely metallic (electrons labeled 1 and 2 in Fig. 2, 2 in Fig. 3) or purely atomic (electron labeled 1 in Fig. 3). We are thus neglecting the cross product terms which arise when the true wave functions of electrons participating in a sort of combined process are used. An electron whose energy is near that of the metastable level outside the metal should be represented by a wave function which is partly inside the metal and partly in the atom. The integrated ratio of the probability of finding the electron in the metastable level to that of finding it inside the metal is taken here to be the ratio of the probability of Auger de-excitation to the probability of Auger neutralization.

XII. EFFECTS WHICH BROADEN THE ELECTRON ENERGY DISTRIBUTION

We proceed now to include specifically in the theory those effects which broaden the energy distribution function, $N_i(\epsilon_k)$. We expect the true $N_i(\epsilon_k)$ functions to be broader than those shown in Figs. 10, 11, and 14 by virtue of the following:

1. E_i' is a function of s and $P_t(s,v_0)$ has finite width on the s scale, and,
2. the initial and final states of the process have finite lifetimes.

For the case of Auger neutralization the energy distribution $N_i(\epsilon_k)$ is obtained from expression (19) by use of $P_k(\epsilon_k,s)$ from (18). This gives

$$N_i(\epsilon_k)=N(\epsilon_k)\int_0^\infty \frac{P_t(s,v_0)T[(\epsilon_k+\epsilon_0-E_i')/2]ds}{\int_{\epsilon_F}^\infty N(\epsilon_k)T[(\epsilon_k+\epsilon_0-E_i')/2]d\epsilon_k}, \quad \epsilon_k>\epsilon_F$$
$$=0, \quad \epsilon_k<\epsilon_F. \tag{71}$$

If one puts into this expression $E_i'(s)$ from Eq. (65), for example, the first cause of broadening listed above is then included in the theory although the calculation indicated is prohibitively tedious. We simplify expression (71) by assuming the integral over ϵ_k in the denominator to be independent of s and by writing

$$E_i'(s)=E_i'(s_m)+k(s-s_m), \tag{72}$$

where k is $[dE_i'/ds]_{s=s_m}$. Then we may write

$$N_i(\epsilon_k)\propto N(\epsilon_k)\int_0^\infty P_t(s,v_0)T[(\epsilon_k+\epsilon_0-E_i'(s_m)-k(s-s_m))/2]ds. \tag{73}$$

The second cause of broadening listed above, namely that due to finite lifetimes, is included as follows. The lifetime in the initial state is determined by the transition rate $R_t(s)$ if we assume only one process to be of importance in the range of s over which the $P_t(s,v_0)$ function has value. The final state has a finite lifetime because the electrons participating in the Auger ejection process leave holes in the filled portion of the conduction band which are filled by secondary Auger processes involving electrons lying higher in the band. These secondary processes are the same as those proposed by Skinner[35] to account for the observed tailing at the long wavelength limit in the soft X-ray spectra of metals. Landsberg[36] has calculated the broadening by these secondary Auger processes and has shown it to be zero when the holes lie at the top of the filled band [$\epsilon'=\epsilon''=\epsilon_F$ in the present case; see Fig. 4] and maximum when the holes lie at the bottom of the band [$\epsilon'=\epsilon''=0$]. Thus tailing at the low-energy limit of the $N_i(\epsilon_k)$ distribution is caused by the finite lifetimes in both initial and final states whereas that at the high-energy limit results from initial state lifetime only. Broadening of the $N_i(\epsilon_k)$ function at lower ϵ_k is difficult to observe in the experimental $N_0(E_k)$ curves because it is largely obscured by the effects of the probability of escape and target-collector geometry. The high-energy tail of the $N_0(E_k)$ function, on the other hand, resembles closely that of the $N_i(\epsilon_k)$ function because $P_e(\epsilon_k)$ is relatively slowly varying at larger ϵ_k. For this reason experimental observations concerning the high-energy tail only are used in the theory and broadening due to the finite lifetime of the initial state only is incorporated in the theory.

The elemental Auger transition, for which ϵ', ϵ'', and s have specific values, results in excited electrons whose energies may be taken to be distributed according to the function[37]

$$I(\delta,s)=1/[\delta^2+(\hbar R_t(s)/2)^2], \tag{74}$$

in which δ is the energy difference from the nominal ϵ_k for the process and $R_t(s)$ is the rate function. A corresponding spread in the translational energy of the atom is demanded by the conservation of energy. The expression for $N_i(\epsilon_k)$ which takes account of both types of

[35] H. W. B. Skinner, Phil. Trans. Roy. Soc. (London) **A239**, 95 (1940).
[36] P. T. Landsberg, Proc. Phys. Soc. (London) **A62**, 806 (1949).
[37] This is the natural line profile discussed, for example, in Sec. 18 of W. Heitler, *The Quantum Theory of Radiation* (Oxford University Press, London, 1954), third edition.

broadening is thus

$$N_i(\epsilon_k) \propto N(\epsilon_k) \int_{-\infty}^{\infty} \int_{0}^{\infty} P_t(s,v_0) I(\delta,s) \times T[(\epsilon_k+\delta+\epsilon_0-E_i'(s_m)-k(s-s_m))/2] ds d\delta. \quad (75)$$

We further simplify expression (75) by evaluating $I(\delta,s)$ at $s=s_m$ and by approximating P_t and I by Gaussian distributions $\Phi_{\sigma 1}$ and $\Phi_{\sigma 2}$ having widths at half-maximum equal to those of P_t and I, respectively. Thus we replace the double integral in (75) by

$$T_\sigma(\epsilon_m) = \int_{-\infty}^{\infty} \int_{-\infty}^{\infty} \Phi_{\sigma 1}(y) \Phi_{\sigma 2}(z) T(\epsilon_m+y+z) dy dz = \int_{-\infty}^{\infty} \int_{-\infty}^{\infty} \Phi_\sigma(x) T(\epsilon_m+x) dx, \quad (76)$$

in which

$$\epsilon_m = [\epsilon_k+\epsilon_0-E_i'(s_m)]/2, \quad (77)$$

$$y = \delta/2, \quad (78)$$

$$z = -k(s-s_m)/2 = -(1/2)(s-s_m)[dE_i'/ds]_{s=s_m}, \quad (79)$$

$$\Phi_\sigma(x) = [1/\sigma(2\pi)^{\frac{1}{2}}] \exp(-x^2/2\sigma^2), \quad (80)$$

and

$$\sigma = (\sigma_1^2+\sigma_2^2)^{\frac{1}{2}}. \quad (81)$$

The limits of integration over z in (76) are taken as $-\infty$ to ∞ in place of $-\infty$ to $ks_m/2$ because $P_t(s,v_0)$ is essentially zero in the range $ks_m/2<z<\infty$. The T function in (76) is given in (15). Thus, finally,

$$N_i(\epsilon_k) = \frac{N(\epsilon_k) T_\sigma[(\epsilon_k+\epsilon_0-E_i'(s_m))/2]}{\int_{\epsilon_F}^{\infty} N(\epsilon_k) T_\sigma[(\epsilon_k+\epsilon_0-E_i'(s_m))/2] d\epsilon_k}. \quad (82)$$

In this expression $N_i(\epsilon_k)$ is normalized to an area of one electron per incident ion for the reasons discussed in Secs. III and XIII.

The widths at half-maximum, $W(\Phi_{\sigma 1})$ and $W(\Phi_{\sigma 2})$, of the functions $\Phi_{\sigma 1}$ and $\Phi_{\sigma 2}$, respectively, are evidently

$$W(\Phi_{\sigma 1}) = (1/2) W(P_t)[dE_i'/ds]_{s=s_m} = (1.25/a)[dE_i'/ds]_{s=s_m}, \quad (83)$$

from (79) and (42), and

$$W(\Phi_{\sigma 2}) = \hbar R_t(s_m) = \hbar a v_0, \quad (84)$$

from (74), (35), (40), and the simplification of evaluating $I(\delta,s)$ at $s=s_m$.

The relation of the parameter σ in the Gaussian distribution (80) to the width $W\Phi_\sigma$) at half-maximum is

$$\sigma = W(\Phi_\sigma)/2.37, \quad (85)$$

from which it follows that

$$\sigma_1 = (0.53/a)[dE_i'/ds]_{s=s_m}, \quad (86)$$

and

$$\sigma_2 = 0.42 \hbar a v_0. \quad (87)$$

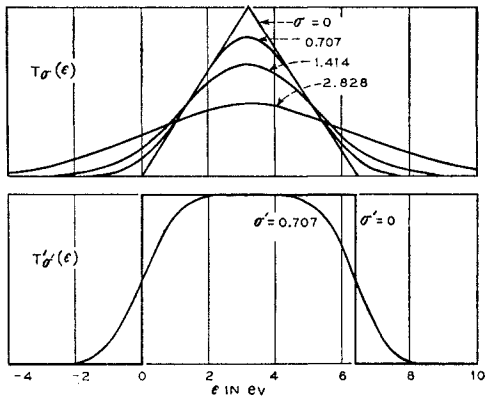

FIG. 26. Plots of $T_\sigma(\epsilon)$ and $T_{\sigma'}(\epsilon)$ functions for $N_c(\epsilon)=$ constant (k_1) and for several choices of the parameters σ and σ'. Analytic expressions for these functions are to be found in Table III.

The procedure to be followed to determine a broadened $N_i(\epsilon_k)$ function for Auger neutralization is then the following:

1. Calculate the Auger transform $T(\epsilon)$ from Eq. (15) assuming a state density function $N_c(\epsilon)$.

2. Calculate the broadened Auger transform $T_\sigma(\epsilon_m)$ from (76) using (77), (80), (81), and σ_1 and σ_2 parameters from (86) and (87). This involves a fit to the experimental data to get σ_1 as discussed in the next section.

3. Shift $T_\sigma(\epsilon_m)$ on the energy axis as indicated in (82), multiply by $N(\epsilon_k)$, and normalize to unity area. In this step a final state density function $N(\epsilon_k)$ proportional to $\epsilon_k^{\frac{1}{2}}$ has been assumed.

The broadening of the $N_i'(\epsilon_k)$ distribution for Auger de-excitation may be treated in a manner entirely analogous to that just discussed for Auger neutralization. By carrying through the argument using the results of Sec. IV it can be shown that

$$N_i'(\epsilon_k) = \frac{N(\epsilon_k) T_{\sigma'}'[\epsilon_k - E_x'(s_m')]}{\int_{\epsilon_F}^{\infty} N(\epsilon_k) T_{\sigma'}'[\epsilon_k - E_x'(s_m')] d\epsilon_k}, \quad \epsilon_k > \epsilon_F = 0, \quad \epsilon_k < \epsilon_F, \quad (88)$$

where

$$T_{\sigma'}'(\epsilon_m') = \int_{-\infty}^{\infty} \Phi_{\sigma'}(x) N_c(\epsilon+x) dx \quad (89)$$

and

$$\epsilon_m' = \epsilon_k - E_x'(s_m').$$

σ' is again $(\sigma_1'^2+\sigma_2'^2)^{\frac{1}{2}}$, where now

$$\sigma_1' = (1.06/a)[dE_x'/ds]_{s=s_m'}, \quad (90)$$

and

$$\sigma_2' = 0.42 \hbar a' v_0. \quad (91)$$

Analytic expressions for the $T(\epsilon)$, $T'(\epsilon)$, $T\sigma(\epsilon)$ and $T_{\sigma'}'(\epsilon)$ functions are listed in Table III for some choices of $N_c(\epsilon)$. $T_\sigma(\epsilon)$ and $T_{\sigma'}'(\epsilon)$ for $N_c(\epsilon)=k_1$ are plotted in Fig. 26 for several choices of σ and σ'.

XIII. FITS TO THE EXPERIMENTAL DATA AND CONCLUSIONS CONCERNING THE MATRIX ELEMENT

With the determination of the broadened $N_i(\epsilon_k)$ function in the last section the theory of Auger ejection to be presented here has been completed inasmuch as the $N_0(E_k)$ distribution may be determined from N_i and the escape probability, and the total external yield as the integral over N_0. We wish now to apply this theory to the specific cases of the singly charged ions of the noble gases incident on clean tungsten which have been studied recently experimentally.[7] Since resonance neutralization is impossible for He^+, Ar^+, Kr^+, and Xe^+ at a clean tungsten surface (Sec. X) we expect these ions to eject electrons by the process of Auger neutralization only. In this section we estimate or determine by fits to the experimental data the unknown parameters in the theory of Auger neutralization. The role played by Auger de-excitation in the case of Ne^+ on clean tungsten and what is learned about the process from fitting the theory to the experimental data are discussed in the next section.

We now discuss the basic functions which we need before the theory of Auger neutralization can be applied.

1. The state density function, $N_c(\epsilon)$, is needed to determine the Auger transform, $T(\epsilon)$, by Eq. (15). We have taken $N_c(\epsilon)=$constant as the best approximation to the function calculated by Manning and Chodorow[24] (see Figs. 8 and 9 and Sec. VII).

2. We also need the transition probability per unit time, $R_t(s)=A\exp(-as)$, which specifies the dependence of the matrix element on s. As indicated in Sec. V values of $a=2\times10^{-8}$ cm^{-1} and 5×10^{-8} cm^{-1} have been used. A is determined from the experimental data by fitting to the high-energy tail of the experimental $N_0(E_k)$ curves in the following way. The tangent line through the point of inflection on the high-energy side of experimental $N_0(E_k)$ distribution is extrapolated to the $E_k(e^-)$ axis (see He^+ curve in Fig. 7 of the accompanying paper).[7] This intercept is taken to give a reasonable value for $E_i'(s_m)-2\varphi$. That this should be so is to be seen by comparing the $N_i(\epsilon_k)$ distributions labeled 2 and 3 in Fig. 4. Here curve 2 is the unbroadened distribution resulting from transitions all of which occur at $s=s_m$. Curve 3 is the broadened $N_i(\epsilon_k)$ distribution. It is evident that curve 2 approximates a tangent through the point of inflection of curve 3 on the high energy side. Point a, which is the maximum energy in the distribution 2 and thus approximately the position of the intercept of the line tangent to 3, lies at $E_i'(s_m)-2\varphi$. The value $E_i'(s_m)$ determined in this way may be used with the appropriate curve of Fig. 23 to give a value of s_m (Table VIII). This, by Eq. (40), specifies the parameter A, when a and v_0 are known. The values of A found in this way are listed in Table IX. Transition rate parameters to be found in the literature are listed in Table X. For convenience, velocities of noble gas ions for various incident kinetic energies of interest are listed in Table XI.

3. Finally, we need the probability distribution $P_\Omega(\theta,\epsilon_k)$ which gives the θ dependence of the matrix element. On the basis of the assumptions discussed in Sec. VI, $P_\Omega(\theta,\epsilon_k)$ is determined by the parameter f which specifies the ratio of matrix elements for processes yielding escaping and internally reflected excited electrons. f is determined by fitting the theoretical γ_N for He^+ ions of 40 ev incident energy to the experimental value of 0.282. This procedure yields $f=2.2$ and the escape probability function plotted as curve 2 in Fig. 7. Whereas we determine a value of the parameter A for each noble gas ion we use the same value of f for all.

In addition to the above functions we need values of the σ_1 and σ_2 parameters which determine the broadening of the $N_i(\epsilon_k)$ distribution. By Eq. (86) σ_1 depends on the parameter a and $[dE_i'/ds]_{s=s_m}$, which may be determined from Fig. 23 or Eq. (65) using the s_m value determined above. By Eq. (87), σ_2 is calculable directly from a and v_0. σ_1, σ_2, and the resulting σ are listed in Table VIII for each choice of the parameter a.

By virtue of the two fits to the experimental results which yield values of the parameters A and f we have in effect determined the two basic characteristics of the matrix element, namely its dependence on s and θ, which an evaluation of the matrix element from first principles would be expected to supply. Although there is nothing in previous calculations with which to compare the value $f=2.2$, it appears to be reasonable. On the other hand, the values for A determined in this work are much larger than those calculated by Shekhter[3] and Cobas and Lamb.[4] In the light of the present work these earlier values look much too low. For 40-ev

TABLE VIII. Parameters which characterize Auger neutralization by 40-ev ions.

Ion	$E_i'(s_m)$ (ev)	s_m (A)	$a=2\times10^8$ cm^{-1} σ_1 (ev)	σ_2 (ev)	σ (ev)	$a=5\times10^8$ cm^{-1} σ_1 (ev)	σ_2 (ev)	σ (ev)
He^+	22.6	2.2	0.63	0.244	0.69	0.25	0.61	0.66
Ne^+	19.6[a]	2.4	0.63	0.108	0.64	0.25	0.27	0.37
Ar^+	14.0	3.0	0.63	0.080	0.64	0.25	0.20	0.32
Kr^+	12.3	3.2	0.63	0.056	0.63	0.25	0.14	0.29
Xe^+	10.6	3.6	0.63	0.044	0.63	0.25	0.11	0.27

[a] Since $E_i'(s_m)-2\varphi$ cannot be obtained from the experimental curve for Ne^+ at 40 ev because of the tail due to Auger de-excitation, this value has been determined from the intersection with the Ne curve of the locus of $E_i-E_i'(s_m)$ values for 40-ev ions in Fig. 23.

TABLE IX. Transition rate parameters for Auger neutralization from the present work.

	A (sec^{-1}) $a=2\times10^8$ cm^{-1}	$a=5\times10^8$ cm^{-1}
He^+	7.1×10^{16}	1.5×10^{20}
Ne^+	4.8×10^{16}	1.6×10^{20}
Ar^+	1.1×10^{17}	2.3×10^{21}
Kr^+	1.2×10^{17}	4.6×10^{21}
Xe^+	2.1×10^{17}	2.5×10^{22}

TABLE X. Summary of published transition rate parameters.

	Auger processes					
	Neutralization		De-excitation		Resonance processes	
	A (sec^{-1})	a (cm^{-1})	A' (sec^{-1})	a' (cm^{-1})	A'' (sec^{-1})	a'' (cm^{-1})
Shekhter[c]	6.35×10^{14} [a]	3.9×10^{8} [a]			5.74×10^{19}	3.2×10^{8}
Cobas and Lamb[d]			9.6×10^{16}	7.3×10^{8}	9.1×10^{18} [b]	1.9×10^{8} [b]

[a] Evaluated by expanding in Taylor's series the polynomial in Shekhter's expression for $R_t(s)$ [his Eq. (3.11)] about the point $s=2.2$ A.
[b] Evaluated by expanding in Taylor's series the polynomial in Cobas and Lamb's expression for $R_t''(s)$ about the point $s=5.0$ A.
[c] See S. S. Shekhter (see reference 3).
[d] See A. Cobas and W. E. Lamb (see reference 4).

He^+ ions Shekhter's parameters A and a give $s_m<0$. Cobas and Lamb's values for A' and a' give $s_m'=0.47$ A for 40-ev He^m. It is clear that if the variation of atomic energy levels near the metal is anything like that derived in this paper one cannot produce with the theory the form of $N_0(E_k)$ observed in the experiment for such low values of A. The observed $N_0(E_k)$ distributions are so nearly like those calculated for no variation of energy levels (e.g., Fig. 12) that the $P_t(s,v_0)$ function must lie at distances from the surface where only relatively small displacements of the energy levels have occurred. This is thought to be a fairly important and direct conclusion. The specific range of A values which this indicates does depend upon the details of the potential curves used in Sec. IX and upon the distance scale prescribed by the procedures of Sec. VIII. But it is evident that the rate functions calculated thus far from first principles make it necessary that the process occur very close to the surface and this seems difficult to reconcile with the experimental observations.

It is difficult to put a finger on the reason for the low values of A calculated from direct evaluation of the matrix element. Cobas and Lamb's A' value should be low inasmuch as they took the wave functions of metal electrons to be zero outside the metal. However, Shekhter, who retained the tails outside the metal, calculated a smaller transition rate than did Cobas and Lamb. In this connection it is interesting to note that the parameters for resonance neutralization calculated by Shekhter and by Cobas and Lamb (Table X) give $s_m''=3.3$ A and 4.9 A, respectively. These are not far from what one would think reasonable in the light of the Ne^+ results. Finally, it should be noted in Table IX how profoundly the choice of a affects the value of A.

Fixing A at the values given in Table IX may now be seen to justify the assumption made earlier that $\int_0^\infty P_t(s,v_0)ds\cong1$ or the equivalent statement that $\int_0^\infty N_i(\epsilon_k)d\epsilon_k\cong1$ electron per incident ion. For the least favorable case in Table IX (He^+: $a=2\times10^{-8}$ cm^{-1}, $A=7.1\times10^{16}$ sec^{-1}) we find $\int_0^\infty P_t(s,v_0)ds\cong1-\exp(-81)$ by Eq. (48). Another way of stating the high probability of the Auger transition occurring on the inward trip of the ion is that $\int_s^\infty P_t(s,v_0)ds>0.999$ at $s=s_m-1$A for $a=2\times10^{8}$ cm^{-1} or $s=s_m-0.4$ A for $a=5\times10^{-8}$ cm^{-1}. With the relatively large values of s_m given in Table VIII it follows that at 40 ev essentially all ions will have participated in an Auger transition before the ion gets close enough for other means of its neutralization to become operative. These conclusions are in agreement with the observation of very low reflection of ions as ions or as metastable atoms at low incident kinetic energy.

XIV. THEORETICAL ELECTRON ENERGY DISTRIBUTIONS AND ELECTRON YIELDS

We are now in a position to construct theoretical electron energy distributions which include the effects of atomic energy level variation near the metal and the Heisenberg principle. For He^+, Ar^+, Kr^+, and Xe^+, since Auger neutralization only is possible, $N_i(\epsilon_k)$ distributions are obtained from Eq. (82) using Manning and Chodorow's calculated value of $\epsilon_F=6.4$ ev, $\epsilon_0=\epsilon_F+\varphi=10.9$ ev, and the values of $E_i'(s_m)$ given in Table VIII. To avoid lengthy computation a single value of σ equal to 0.707 has been used for all ions. The $N_i(\epsilon_k)$ functions obtained in this way are plotted in Fig. 27. The distribution in energy of external secondary electrons, $N_0(E_k)$, is obtained from the $N_i(\epsilon_k)$ function in each case by multiplying by the escape probability, $P_e(\epsilon_k)$, of Eq. (55) with $f=2.2$ (curve 2 of Fig. 7). These curves are plotted in Fig. 28. Total electron yields determined as areas under these $N_0(E_k)$ distributions are listed in Table XII where are also listed the experimental values for comparison.

It is evident that the high-energy tail of the experimental $N_0(E_k)$ curve for Ne^+ cannot be simulated if electrons are ejected only in the process of Auger neutralization (dashed curve in Fig. 28). It has been seen, however, that resonance neutralization is possible for Ne^+ at a clean tungsten surface (Sec. X) and that Auger de-excitation of Ne^m can produce electrons of energies outside the metal greater than can arise in Auger neutralization (Sec. IX). By virtue of these facts it has been possible to construct a distribution for electrons from Ne^+ on tungsten which resembles the experimentally observed one. It is compounded of $N_i(\epsilon_k)$ and $N_i'(\epsilon_k)$ functions in the manner $f_NN_i(\epsilon_k)+(1-f_N)N_i'(\epsilon_k)$, where f_N is the fraction of incident ions which finally decay by Auger neutralization and N_i and N_i' are the distributions for Auger neutralization and de-excitation, respectively, each normalized to an area of one electron per incident ion.

In order to calculate a broadened $N_i'(\epsilon_k)$ function it is evident that we need to know σ_1', σ_2', $E_x'(s_m')$, s_m'.

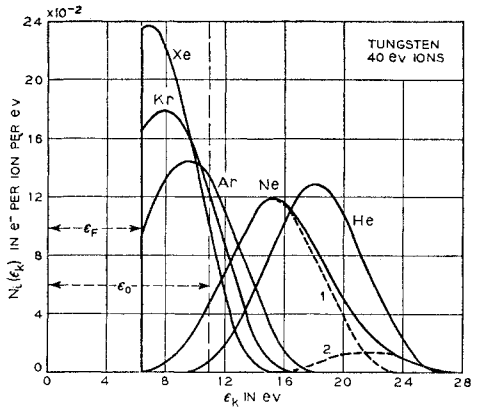

FIG. 27. Theoretical $N_i(\epsilon_k)$ distributions for 40-ev ions incident on clean tungsten determined from the theory which includes effects of the variation of energy levels near the metal and the Heisenberg uncertainty principle. For He^+, Ar^+, Kr^+, and Xe^+ the electrons come from the process of Auger neutralization. For Ne^+ *ca* 90 percent of the electrons arise in Auger neutralization (curve 1), 10 percent in Auger de-excitation (curve 2) as explained in the text.

Assuming the rate functions $R_t(s)$ and $R_t'(s)$ to be equal (Sec. V) means that $s_m'=s_m$, $a'=a$, and thus $\sigma_2'=\sigma_2$. Evaluation of σ_1' by Eq. (90) involves more detailed knowledge of $E_x'(s)$ than we possess, and no attempt to evaluate σ_1' has been made. In finding $T_{\sigma'}'(\epsilon)$ it is perhaps reasonable to use $\sigma'=0.707$, the same value as that used for σ in finding $T_\sigma(\epsilon)$. The $T_{\sigma'}'(\epsilon)$ functions for $\sigma'=0$ and 0.707 are plotted in Fig. 26. We have used the same escape probability function for the de-excitation process as for the neutralization process, i.e., $P_e'=P_e$. This means that we assume the same ratio f of matrix elements in the two cases, a not unreasonable assumption for the exchange de-excitation process.

After some trial and error it has been found that the experimentally observed tail on the $N_0(E_k)$ curve for Ne^+ at 40 ev can be closely approximated with $E_x'(s_m')-E_x=2.5$ ev and $f_N=0.9$. This value of $E_x'(s_m')$ is a little less than that indicated in Fig. 22 for $s_m'=2.4$ A ($s_m'=s_m$ taken from Table VIII). Another method of determining f_N is based on the fact that the total yield for the combined process may be written as

$$\gamma_i=f_N\gamma_N+(1-f_N)\gamma_D. \tag{92}$$

Values for γ_N and γ_D values equal to 0.208 and 0.340, respectively, have been calculated by using $E_i'(s_m)=19.6$ ev, $E_x'(s_m')-E_x=2.5$ ev, and $P_e'=P_e$. A value of f_N may now be determined which makes the γ_i of (92) equal the experimentally observed value of 0.232 at $E_k(Ne^+)=40$ ev. The value $f_N=0.82$ found in this way is in reasonable agreement with the value 0.9.

It is evident that a high value of f_N is indicated by the experiment. This requires that the critical distance s_c lie in the range of s in which the $P_t''(s,v_0)$ function for the resonance process in Ne has value for ion energies near 100 ev. The two-stage process of electron ejection is thus much less important for ions of the noble gases incident on clean metals than has formerly been supposed.

We may now compare the theoretical and experimental results for γ_i and $N_0(E_k)$. Table XII indicates that the trend of γ_i is predicted and, in fact, with reasonable accuracy, the magnitudes themselves, once the fit for He^+ has been made. Comparison of Fig. 28 with Fig. 7 of the accompanying paper[7] shows the general forms of the $N_0(E_k)$ distributions, in particular the high-energy tails, to be reproduced quite well also. The deficiency of slow electrons observed for He^+ is evidently to be understood as resulting from the fact that $E_i'-2\epsilon_0>0$ for this ion at the values of s where the process occurs. Even though the relative maxima of the $N_0(E_k)$ distributions observed for He^+ and Ne^+ are not reproduced by the theory, the relative γ_i values are quite good in spite of the complication with Auger de-excitation for Ne^+. For Ar^+, Kr^+, and Xe^+, on the other hand, the theory gives γ_i values which are clearly too low. This is not too surprising inasmuch as we espect the results for these ions to be much more sensitive to the specific choices made for $N_c(\epsilon)$, $F(\epsilon',\epsilon'')$ and P_Ω, and thus to the form of the $N_i(\epsilon_k)$ distribution, than are the results for He^+ and Ne^+. This arises from the fact that only those electrons lying in the high-energy tail of the $N_i(\epsilon_k)$ distribution for Ar^+, Kr^+, and Xe^+ have any chance of leaving the metal whereas for He^+ and Ne^+ essentially the whole of the $N_i(\epsilon_k)$ distribution lies at $\epsilon_k>\epsilon_0$. Furthermore, the use of the same f parameter in determining $P_\Omega(\theta,\epsilon_k)$ and $P_e(\epsilon_k)$ for all ions may introduce some error.

It is interesting to note the effect of the choice of the parameter a in the rate function $R_t(s)$. Table VIII indicates that for $a<2\times10^8$ cm^{-1} $\sigma\simeq\sigma_1$ and the broadening of $N_i(\epsilon_k)$ is determined entirely by the variation in E_i' over the values of s at which the process occurs [Eq. (86)]. For $a>5\times10^8$ cm^{-1} $\sigma\simeq\sigma_2$ and broadening is governed only by the Heisenberg principle [Eq. (87)]. In the latter case σ depends upon v_0 and thus varies from ion to ion at a given energy. That this is perhaps more in agreement with experiment than is a constant σ is indicated in the next section. Values of σ obtained for values of a much outside the range 2 to 5×10^8 cm^{-1} appear to be so large as to make difficult a good prediction of the forms of the high-energy tails of the $N_0(E_k)$ distributions.

TABLE XI. Velocities of noble gas ions.

Ion	$10^{-6}\times$velocity in cm/sec. $E_k=1$ ev	$E_k=40$ ev	$E_k=200$ ev	$E_k=1000$ ev
He^+	0.70	4.38	9.8	21.9
Ne^+	0.32	1.96	4.38	9.8
Ar^+	0.22	1.39	3.11	6.95
Kr^+	0.16	0.96	2.15	4.8
Xe^+	0.13	0.77	1.72	3.85

XV. VARIATIONS WITH ION KINETIC ENERGY

To a first, rather crude approximation Auger ejection of electrons from metals is independent of incident ion energy in both experiment and theory. The smaller variations observed in the study of tungsten,[7] however, present something of a challenge to any theory of the phenomenon. The observed variations of γ_i with incident ion energy are: 1. the drop in $\gamma_i(He^+)$ at ion energies up to 400 ev, 2. the rise in $\gamma_i(He^+)$ above 400 ev, 3. the rise in $\gamma_i(Ne^+)$ in the range of 10 to 100 ev and the levelling off at higher energies, 4. the slow rise in γ_i of Ar^+, Kr^+, and Xe^+ with increasing ion energy. The main effect of increasing ion energy on the electron energy distributions, $N_0(E_k)$ is to lengthen the high-energy tail. The increase in the relative proportion of slow electrons observed in the case of He^+ is also of interest.

In considering variations with ion kinetic energy from the point of view of theory we shall discuss first the cases of pure Auger neutralization, namely, those for He^+, Ar^+, Kr^+, and Xe^+. The theory predicts variation of γ_i and form of $N_0(E_k)$ through the effects of variation of energy levels near the metal surface and the Heisenberg uncertainty principle. As the incident velocity of the ion is increased, s_m decreases by Eq. (40), but the form of the $P_t(s,v_0)$ function remains invariant. This means that for higher incident velocities the Auger transitions take place closer to the metal. There are two results of faster ion approach and the consequent neutralization closer to the metal which then determine the variation of γ_i and $N_0(E_k)$. These are:

1. The effective ionization energy is smaller for transitions occurring closer to the metal (see Figs. 4 and 23).

2. The broadening of the $N_i(\epsilon_k)$ distribution is greater both because of the increase of dE_i'/ds, which increases σ_1 [Eq. (86)], and because of the increase of σ_2 with incident velocity [Eq. (87)].

Reduction of $E_i'(s_m)$ can be seen by Eq. (82) to shift the $N_i(\epsilon_k)$ distribution to lower values of ϵ_k, the final effect of which is to reduce γ_i. We may look upon the effect of greater broadening of the $N_i(\epsilon_k)$ distribution, somewhat crudely, as removing electrons from the middle of the distribution and placing half of these in the high-energy and half in the low-energy tails. The effect of this upon γ_i depends upon where, with respect to the level $\epsilon_k=\epsilon_0$, the $N_i(\epsilon_k)$ distribution lies. For He^+ the $N_i(\epsilon_k)$ distribution lies essentially entirely at $\epsilon_k>\epsilon_0$ (Fig. 27). Here broadening of the distribution results in reducing γ_i because electrons in the enlarged low-energy tail never leave the metal. On the other hand, for a distribution $N_i(\epsilon_k)$ of which only a portion near the high-energy end lies at $\epsilon_k>\epsilon_0$, broadening of the distribution increases γ_i because there are more electrons in the high-energy tail which can leave the metal. The observed variation in γ_i is thus a combination of effects due to energy level variation and distribution broadening, both of which decrease γ_i for He^+ but have opposite effects on γ_i for the heavier ions.

In Fig. 29 are shown $N_i(\epsilon_k)$ distributions calculated for He^+ and Kr^+ ions of 40-, 200-, and 1000-ev incident energy. The values of $E_i'(s_m)$ at 40 ev are those given in Table VIII. $E_i'(s_m)$ values at 200 and 1000 ev are determined from Fig. 23 using values of s_m calculated by Eq. (40) with $a=5\times10^8$ cm^{-1} and the corresponding values of A given in Table IX.

For simplicity of calculation, the values 0.707, 1.414, and 2.828 have been used for σ at 40, 200, and 1000 ev, respectively, in determining the $N_i(\epsilon_k)$ functions of

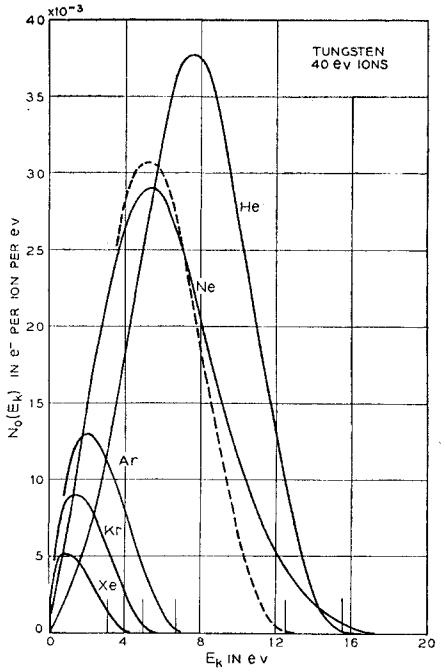

FIG. 28. Theoretical $N_0(E_k)$ distributions for 40 ev ions determined from the theory which includes effects of the variation of energy levels near the metal and the Heisenberg uncertainty principle. These curves have been obtained from the $N_i(\epsilon_k)$ distributions of Fig. 27 using the $P_e(\epsilon_k)$ function of Eq. (55) with $f=2.2$. The energy limits $E_i-2\varphi$ are indicated by the vertical lines above the E_k axis. The dashed curve for Ne indicates what $N_0(E_k)$ for this ion would be if all Ne^+ ions decayed finally via Auger neutralization. Thus it is obtained from an $N_i(\epsilon_k)$ distribution like curve 1 of Fig. 27 which is normalized to unity area.

TABLE XII. Theoretical and experimental electron yields for 40 ev ions.

Ion	Calculated yield[a]	Measured yield
He^+	0.279	0.282
Ne^+	0.220[b]	0.232
Ar^+	0.050	0.097
Kr^+	0.027	0.048
Xe^+	0.012	0.017

[a] The calculation of these γ_i values involves a fit to the data for He^+ only from which fit the parameter $f=2.2$ has been determined.
[b] This is the value calculated assuming $f_N=0.9$, that is, using the composite $N_i(\epsilon_k)$ distribution of Fig. 27.

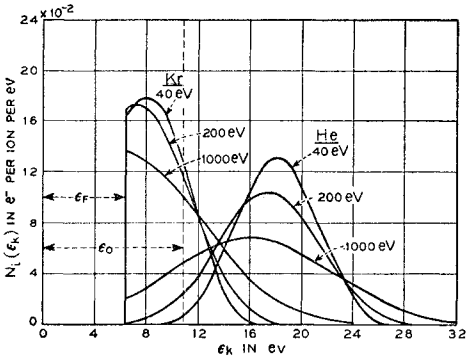

FIG. 29. Theoretical $N_i(\epsilon_k)$ distributions for He^+ and Kr^+ on clean tungsten corresponding to incident ion energies of 40, 200, and 1000 ev using σ values of 0.707, 1.414, and 2.828, respectively.

Fig. 29. These values approximate reasonably well those calculated from the equations of Sec. XII using $a=5\times10^8$ cm^{-1}. Table VIII indicates that for $a=5\times10^8$ cm^{-1} the value $\sigma=0.707$ is approximately correct for He^+ but large for the heavier ions. The distributions of Fig. 29 show that as incident energy increases the distribution broadens and its peak shifts to lower ϵ_k by virtue of the decrease in E_i'.

The $N_0(E_k)$ distributions which result from multiplication of the $N_i(\epsilon_k)$ functions of Fig. 29 by P_e from Eq. (55) with $f=2.2$ are shown in Fig. 30. The γ_i values calculated from these curves and other parameters characterizing the calculations are listed in Tables XIII and XIV for He^+ and Kr^+, respectively. Note

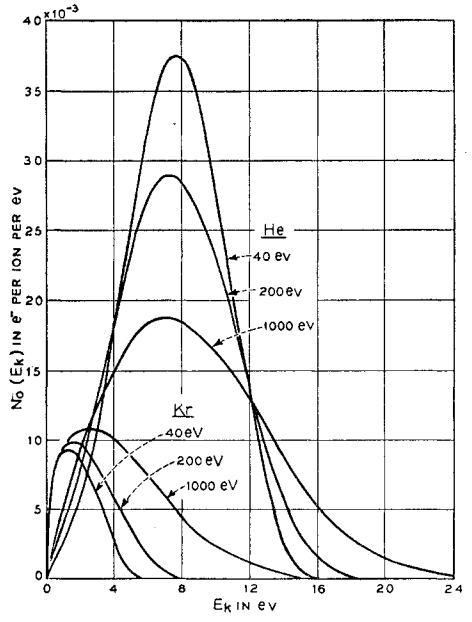

FIG. 30. Theoretical $N_0(E_k)$ distributions for He^+ and Kr^+ of 40, 200, and 1000 ev energy incident on tungsten, obtained from the $N_i(\epsilon_k)$ curves of Fig. 29 by use of the $P_e(\epsilon_k)$ escape probability of Eq. (55) in the text with $f=2.2$. γ_N values derived from these curves are listed in Tables XIII and XIV.

again that the theory is fitted to the experiment only for $\gamma_i(He^+)$ at 40 ev. Since both the effect of reduction in E_i' and increase in broadening is to reduce γ_i for He^+ we find the calculated γ_i in Table XIII reduces steadily with increasing $E_k(He^+)$. For Kr^+, on the other hand, reduction in E_i' reduces γ_i, but broadening increases γ_i. The net result, as the calculated γ_i values of Table XIV show, is to increase γ_i.

Because the σ values used here are perhaps large for Kr^+, a second series of calculations, also listed in Table XIV, were carried out for $\sigma=0$, 0.707, and 1.414 for 40-, 200-, and 1000-ev Kr^+ ions, respectively. The $N_i(\epsilon_k)$ and $N_0(E_k)$ functions for these cases are shown in Fig. 31. The calculated γ_i values first drop and then rise with increasing energy. Comparison with experiment shows that the correct values of σ must lie somewhere between the two sets of values used. This is perhaps evidence that a lies nearer 5×10^8 cm^{-1}, which

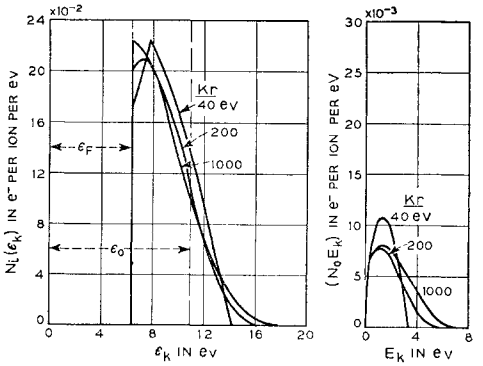

FIG. 31. Theoretical $N_i(\epsilon_k)$ and $N_0(E_k)$ distributions for Kr^+ of 40, 200, and 1000 ev energy incident on tungsten determined using σ values of 0, 0.707, and 1.414, respectively. γ_N values derived from the $N_0(E_k)$ curves are listed in Table XIV.

choice gives σ values which decrease in going from He^+ to Xe^+, than 2×10^8 cm^{-1}, for which choice σ is approximately constant (Table VIII).

For the cases of pure Auger neutralization it is evident that the theory can account for the initial drop in γ_i for He^+ and the slow rise in γ_i for Ar^+, Kr^+, and Xe^+ but cannot account for the rise at higher energies observed for He^+. This latter is thought to be the result of electron ejection by a process other than an Auger process setting in at higher energies. The reasons for this assignment are the following.

1. Other processes are known to set in at greater incident velocities. According to Ploch[8] the most probable of these is the release of bound electrons from surface atoms.

2. The deviation of experiment from what can be explained by the theory of Auger processes is observed first for He^+, the ion having the greatest velocity at a given ion kinetic energy. Ploch believes release of bound electrons from surface atoms to be purely velocity-

dependent for isotopic ions. It is thus not unreasonable to find such electrons first for He^+.

3. The extra electrons released at higher velocities of the ion are predominantly slow electrons which are not to be expected from the Auger process.

The principal effect of increasing ion energy on the form of the $N_0(E_k)$ distribution is to increase the high-energy tail. This is the direct result of the $N_i(\epsilon_k)$ distribution broadening and is to be observed in Figs. 30 and 31. Comparison of the theoretical curves with the experimental results (Figs. 12 and 14 of the accompanying paper)[7] again shows quite good agreement for He^+ and evidence that the true state of affairs for Kr^+ lies between those calculated for the two sets of σ values.

We turn now to discuss the variation of γ_i and $N_0(E_k)$ for the case of Ne^+ on clean tungsten. The evidence already presented makes it appear that the electrons ejected by Ne^+ arise predominantly in Auger neutralization with a small admixture from the two-stage process of resonance neutralization followed by Auger de-excitation. We expect the velocity dependence of the pure Auger neutralization of Ne^+ to lie between the He^+ and Ar^+ cases since a large portion but not all of the $N_i(\epsilon_k)$ distribution lies at $\epsilon_k > \epsilon_0$. γ_N for Ne is thus expected to drop with increasing ion velocity but not as drastically as is observed for He^+. We expect little if any ejection by non-Auger processes below 1000-ev ion energy for Ne^+. This conclusion is borne out by the relatively minor increase in slow electrons with increasing ion energy (see Fig. 13 and discussion in the accompanying experimental paper).[7] The yield γ_D of electrons which arise from pure Auger de-excitation in the case of Ne^+, although larger than γ_N, is also expected to drop with increasing ion velocity for reasons like those given to explain the He^+ case.

By far the largest factor in determining the variation of $\gamma_i(Ne^+)$ with ion energy is the variation of the factor f_N which determines the partition between Auger neutralization and Auger de-excitation. It has been shown in Sec. XI that as ion velocity increases we expect a decrease in f_N, thus an increase in the relative proportion of two-stage electron ejection. Since Auger de-excitation, on the average, produces faster electrons inside the metal than does Auger neutralization a decrease in f_N results in an increase in γ_i. This is proposed as the explanation for the rise in $\gamma_i(Ne^+)$ with velocity observed in the low-velocity range (Fig. 4 of accompanying paper).[7] A more detailed analysis of the variation of f_N with ion velocity, not given in this paper, shows that the required variation can be achieved with reasonable choices of the parameters determining the rate functions for resonance and Auger processes and the critical distance s_c. The final variation of $\gamma_i(Ne^+)$ with ion energy is, of course, a rather complicated averaging of the variations for pure Auger neutralization, pure Auger de-excitation, as well as the factor f_N which determines the relative proportion of the two.

TABLE XIII. Comparison of calculated and experimentally observed variation of γ_i with incident ion energy for He^+ on tungsten.

$E_k(He^+)$ (ev)	s_m (A)	$E_i'(s_m)$ (ev)	σ (ev)	γ_N calculated	γ_i measured
40	2.20	22.6	0.707	0.279	0.282
200	2.02	22.0	1.414	0.254	0.252
1000	1.84	20.6	2.828	0.231	0.253

We expect f_N to be nearly unity for 10-ev ions and, in fact, the experiment (Fig. 11 of the accompanying paper)[7] shows that the tail on the Ne^+ distribution due to Auger de-excitation has disappeared at 10 ev.

The success achieved in accounting for all the observed variations with ion energy makes it appear reasonable that the theory may be used to extrapolate the experimental measurements of γ_i to the near-thermal ion energies of interest in gas discharges. There has long existed a question as to the validity of using γ_i values measured for ions of 10 ev or greater energy in the quantitative consideration of electrical discharges through gases where the ion energies are more nearly 0.1 ev. It is felt that this point may now largely be settled inasmuch as the causes of the variations of γ_i with ion velocity appear to be known.

A first point which should be made concerns the acceleration of the ion toward the surface by the image force. One may calculate the value of s_m for ions which start toward the surface with negligible velocity by eliminating v_0 between the equations $A/av_0 = \exp(as_m)$ [from Eq. (40)] and $mv_0^2/2 = e^2/4s_m$ [from Eq. (56)] and solving graphically for s_m. This yields the values 2.6, 2.8, 3.4, 3.6, 4.0 A for He^+, Ne^+, Ar^+, Kr^+, and Xe^+, respectively. Equation (56) shows that the ions at these distances are moving with energies of 1.4, 1.3, 1.1, 1.0, and 0.9 ev, respectively. Thus ions which start toward the surface with negligible velocity are moving at the distances from the surface at which Auger neutralization takes place with velocities of the order of one-third those which ions of 10-ev incident energy possess. For this reason we expect the γ_i values of very slow ions to differ little from those measured for 10-ev ions. Theoretical estimates made by the methods of Sec. XIV indicate that for He^+ and Ne^+ γ_i values for very slow

TABLE XIV. Comparison of calculated and experimentally observed variation of γ_i with incident ion energy for Kr^+ on tungsten.

$E_k(Kr^+)$ (ev)	s_m (A)	$E_i'(s_m)$ (ev)	σ (ev)	γ_N calculated	γ_i measured
40	3.20	12.3	0.707	0.027	0.048
			0	0.023	
200	3.02	11.8	1.414	0.038	0.051
			0.707	0.021	
1000	2.84	10.5	2.828	0.072	0.059
			1.414	0.026	

ions should be very little (<5 percent) greater than those measured for 10-ev ions. The reason for this is the fact that the $N_i(\epsilon_k)$ distributions for these ions lie almost entirely at $\epsilon_k > \epsilon_0$ and the increase in $E_i'(s_m)$ and decrease in broadening which a decrease in v_0 entails have a small effect. For Ar^+, Kr^+, and Xe^+ the effect upon γ_i is perhaps larger because of the fact that $N_0(E_k)$, being composed of electrons in the high-energy tail of $N_i(\epsilon_k)$, is more sensitive to changes in $E_i'(s_m)$ and broadening. The indications are that γ_i for these ions at very low incident energies are greater than those measured at 10 ev by a factor which is no greater than 1.2. This rise in γ_i must be attributed almost entirely to the increase in $E_i'(s_m)$ with decrease in v_0.

XVI. CONCLUSIONS CONCERNING THE ELECTRONIC BAND STRUCTURE OF THE METAL

It is evident from the discussions of this paper that the characteristics of the Auger ejection processes are intimately bound up with the electronic band structure of the metal. Thus it is of interest to explore the possibilities of using these processes to provide information concerning the band structure of metals. The method has a number of distinct advantages. In the first place, the low-lying vacant energy level, which is provided for the Auger process by the incoming ion, may be varied in energy relative to the conduction band by the use of different ions. This possibility of observing the same process for a series of low-lying levels has turned out to be particularly fruitful. Also, the position of the vacant level in space is known to be just outside the metal surface. Thus these processes are bona fide surface effects which probe, in particular, the energy band structure near the surface. There are, to be sure, disadvantages inherent in the Auger processes which will become evident in the subsequent discussion.

We may look to the study of Auger ejection processes for information concerning the following items: 1. the form of the state density function $N_c(\epsilon)$, 2. the energy levels of the top and bottom of the filled portion of the conduction band, and 3. possible variation of the band near the metal surface.

Although the form of the $N_c(\epsilon)$ function plays a role in determining the form of the electron energy distribution $N_0(E_k)$, it is difficult to work back to $N_c(\epsilon)$ from an experimental $N_0(E_k)$. There are two reasons for this for the case of Auger neutralization. Here the form of $N_0(E_k)$ is determined principally by the Auger transform of $N_c(\epsilon)$ [Eq. (15)] rather than $N_c(\epsilon)$ itself. Figures 8 and 9 show how the transform distorts the state density function. Secondly, it is impossible to disentangle $N_c(\epsilon)$ from the possible variation of the matrix element with energy of the interacting electrons specified by the function $F(\epsilon',\epsilon'')$. However, some information concerning $F(\epsilon',\epsilon'')$ might be gained from the study of metals for which $N_c(\epsilon)$ is known. In the case of tungsten the reasonable agreement obtained between the calculated and observed forms for the $N_0(E_k)$ function for He^+ indicates that the assumptions that $N_c(\epsilon)$ and $F(\epsilon',\epsilon'')$ are constant cannot be seriously in error. It is evident that the form of $N_c(\epsilon)$ is to be judged from the $N_0(E_k)$ distributions for cases, like He^+ on tungsten, in which the $N_i(\epsilon_k)$ function lies entirely at $\epsilon_k > \epsilon_0$ and for which there is no admixture of Auger de-excitation. In such cases the effect of the escape probability on the form of the $N_0(E_k)$ function is minimized.

In the Auger de-excitation process the form of the final $N_0(E_k)$ function depends more directly on the $N_c(\epsilon)$ function, since $T'(\epsilon) = N_c(\epsilon)$. To use this process to study $N_c(\epsilon)$ it is necessary to find a situation in which it occurs without an admixture of Auger neutralization. It may not be impossible to find a metal-ion combination for which an excited level in the atom remains opposite the filled portion of the conduction band to a distance from the metal sufficiently small to allow the Auger de-excitation process to occur before reionization of the neutralized particle becomes possible.

Determination of the energy limits of the filled portion of the conduction band from Auger ejection processes appears to be more promising than determination of the form of $N_c(\epsilon)$. The energy of the top of the filled portion, φ ev below the vacuum level for metals, may be obtained roughly from the maximum energy observable in the $N_0(E_k)$ distribution. This is admittedly crude because of variation of energy levels and broadening of the distribution. A perhaps more sensitive indication of φ is to be obtained from the observations of the occurrence or nonoccurrence of the two-stage ejection process. Here again one must estimate the variation of energy levels to obtain a value of φ. In the case of Ne^+ on tungsten the high value of f_N which is still definitely less than unity indicates that s_c is most probably of the order of the value actually obtained using $\varphi = 4.5$ ev for tungsten. Whereas it is true that much better methods exist for finding the energy level of the top of the filled band in clean metals, it is not unreasonable to suppose that for metals covered with foreign atoms or for semiconductors the method described here may prove useful.

The energy level of the bottom of the filled part of conduction band, lying ϵ_0 ev below the vacuum level, may also be estimated on the basis of the Auger ejection data. If we consider all Auger neutralization processes to proceed at $s = s_m$, the maximum of the $P_t(s,v_0)$ function, a minimum electron energy greater than zero and equal to $E_i'(s_m) - 2\epsilon_0$ should result if $E_i'(s_m) > 2\epsilon_0$. It is difficult to observe this minimum directly because of the broadening of the distribution at its low energy end and because of the effect of target-collector geometry. For cases in which $E_i'(s_m) > 2\epsilon_0$ one should observe a depletion of low-energy electrons in the $N_0(E_k)$ distribution, however. This was observed to be the case for He^+ on tungsten for which the $N_0(E_k)$ curve (Fig. 7 of the accompanying paper)[7] at low energy is seen to lie definitely below those for Ne^+, Ar^+, Kr^+, and Xe^+.

The coincidence of the $N_0(E_k)$ curves for these other ions at low electron energy is what is expected if for these ions $E_i'(s_m) \leq 2\epsilon_0$. These observations are taken as experimental evidence that

$$\tfrac{1}{2}E_i'(s_m)_{\mathrm{Ne}} < \epsilon_0(W) < \tfrac{1}{2}E_i'(s_m)_{\mathrm{He}}. \quad (93)$$

The width of the filled portion of the conduction band, ϵ_F, is then obtained as $\epsilon_0 - \varphi$.

From Fig. 23 it appears that $E_i'(s_m)$ for both He^+ and Ne^+ of 40-ev energy is some two volts less than the corresponding E_i. Using $E_i'(s_m)_{\mathrm{He}} = 22.6$, $E_i'(s_m)_{\mathrm{Ne}} = 19.6$, and $\varphi(W) = 4.5$ ev we find

$$5.3 < \epsilon_F(W) < 6.8 \text{ ev}. \quad (94)$$

The observation of an appreciable depletion of slow electrons for He^+ must mean that $\epsilon_F(W)$ does not lie at or very near the upper bound. It appears unlikely also that $\epsilon_F(W)$ is as low as 5.3 ev, for then the minimum electron energy for He^+ would be 3.0 ev. A value somewhere near the middle of the above range, perhaps within 0.5 ev of the 6.4 value calculated by Manning and Chodorow[24] for tungsten, is indicated. Bearden and Snyder[38] estimate $\epsilon_F(W)$ to be 7.0 ± 0.5 and 6.5 ± 0.5 ev from the widths of the soft x-ray levels resulting from transitions from the conduction band to the L_{II} and L_{III} levels, respectively.

Finally, we discuss the information to be gained from the Auger ejection processes concerning the variation of energy levels inside the metal near the surface. Here admittedly one must compare the experimental results with data from other sources. In the case of tungsten, for example, it has been shown that the Auger processes indicate a φ of 4.5 ev and ϵ_F near 6.4 ev in agreement with other work. From this we must conclude that these values characterize the conduction band in tungsten right up to the surface. In the case of a solid for which the properties of the filled band deep in the lattice are known it is not inconceivable that the results of Auger ejection studies might indicate variations in the band near the surface of the solid.

The author wishes to acknowledge with thanks many helpful discussions with C. Herring, J. J. Lander, K. G. McKay, D. Sternberg, G. H. Wannier, and P. A. Wolff. C. Herring and D. Sternberg have kindly read and criticized the manuscript. Thanks are also due Miss B. B. Cetlin, who carried out the numerical calculations, and Miss M. C. Gray and R. W. Hamming for advice concerning the calculations.

Note added in proof.—The experimental values of γ_i quoted in this paper for Ar^+, Kr^+, and Xe^+ are somewhat too large for the reason given in the note added in proof to the preceding paper, in which note the magnitude of the effect is also given.

[38] J. A. Bearden and T. M. Snyder, Phys. Rev. **59**, 162 (1941)